Transportation Research Part C 154 (2023) 104230

Contents lists available at ScienceDirect

Transportation Research Part C

journal homepage: www.elsevier.com/locate/trc

Safety-critical traffic control by connected automated vehicles

Chenguang Zhao [a], Huan Yu [a,b,*], Tamas G. Molnar [c]

[a] Thrust of Intelligent Transportation, The Hong Kong University of Science and Technology (Guangzhou), Nansha, Guangzhou, 511400, Guangdong, China

[b] Department of Civil and Environmental Engineering, The Hong Kong University of Science and Technology, Clear Water Bay, Hong Kong Special Administrative Region of China

[c] Department of Mechanical and Civil Engineering, California Institute of Technology, Pasadena, CA 91106, USA

ARTICLE INFO

Keywords:
Connected automated vehicle
Mixed traffic
Traffic control
Safety-critical control
Control barrier function
State observer

ABSTRACT

Connected automated vehicles (CAVs) have shown great potential in improving traffic throughput and stability. Although various longitudinal control strategies have been developed for CAVs to achieve string stability in mixed-autonomy traffic systems, the potential impact of these controllers on safety has not yet been fully addressed. This paper proposes *safety-critical traffic control (STC)* by CAVs—a strategy that allows a CAV to maintain safety relative to both the preceding vehicle and the following human-driven vehicles (HVs). Specifically, we utilize control barrier functions (CBFs) to impart collision-free behavior with formal safety guarantees to the closed-loop system. The safety of both the CAV and HVs is incorporated into the framework through a quadratic program-based controller that minimizes deviation from a nominal stabilizing traffic controller subject to CBF-based safety constraints. Considering that some state information of the following HVs may be unavailable to the CAV, we employ state observer-based CBFs for STC. Finally, we conduct extensive numerical simulations – that include vehicle trajectories from real data – to demonstrate the efficacy of the proposed approach in achieving provably safe traffic.

1. Introduction

The efficiency of transportation is largely affected by the smoothness of the traffic flow. As such, highway traffic often suffers from traffic oscillations, in which the vehicles driving on the road undergo repeated deceleration-acceleration motions. These oscillations may even amplify along the road, indicating the so-called *string instability* of traffic, that ultimately leads to stop-and-go traffic congestion. Congestion, on one hand, negatively impacts travel time and fuel consumption. On the other hand, it also poses additional risk of conflict or collision between vehicles, thereby adversely affecting traffic safety. Therefore, significant research efforts have been invested into mitigating the traffic oscillations by stabilizing traffic, and the area of *traffic control* has emerged as a solution.

This work focuses on providing a safety-critical solution to traffic control through regulating the motions of connected automated vehicles (CAVs) traveling in the traffic flow. Our goal is to control the CAVs such that they facilitate string stability for the traffic behind them while also guaranteeing that a safe distance is always kept between the neighboring vehicles. To highlight the need for and the benefits of the proposed approach, we first give a brief overview on the relevant literature on stabilizing traffic controllers and traffic safety.

* Corresponding author.
E-mail address: huanyu@ust.hk (H. Yu).

https://doi.org/10.1016/j.trc.2023.104230
Received 3 January 2023; Received in revised form 16 June 2023; Accepted 18 June 2023
Available online 8 July 2023

1.1. Traffic control by connected automated vehicles

Research work on traffic control first relied on conventional *road-based traffic control* systems, such as ramp-metering or varying speed limits, that regulate traffic on spatially-fixed road segments in a centralized manner (Horowitz et al., 2005; Yu and Krstic, 2019; Zhang et al., 2019; Zhang and Ioannou, 2016). Then, the rapid development of CAV technology has drawn extensive attention to *vehicle-based traffic control* of transportation systems through information sharing and coordination between CAVs (Čičić and Johansson, 2018; Čičić et al., 2022; Molnár et al., 2021; Stern et al., 2018; Talebpour and Mahmassani, 2016; Zheng et al., 2015, 2016). Vehicle-based traffic controllers rely on regulating the driving behavior of CAVs, through which the smoothness and throughput of traffic is positively impacted. These distributed, vehicle-based traffic control techniques are the main focus of our work.

There exist several linear and nonlinear feedback control strategies for regulating the motions of CAVs, that rely on various topologies in vehicle-to-vehicle (V2V) communication, different levels of automation on CAVs, and various formation geometries of multiple CAVs (Li et al., 2017b). Early studies focused on *adaptive cruise control (ACC)* (Marsden et al., 2001) that automatically adjusts the speed of automated vehicles to maintain a safe distance from the preceding vehicle. Extended from ACC, *cooperative adaptive cruise control (CACC)* (Milanés et al., 2013; Alam et al., 2014) was developed to control platoons of CAVs by leveraging V2V connectivity. CACC frameworks include, for example, linear feedback controllers that mitigate disturbances in the platoon (Milanés et al., 2013) and model predictive controllers that also guarantee safe distances between adjacent vehicles (Massera Filho et al., 2017). Furthermore, control strategies were also proposed for a single CAV instead of an entire platoon, such as the framework of *connected cruise control (CCC)* (Orosz, 2016).

Despite the promising future envisioned for fully connected and automated traffic systems, a long transition period is inevitable in which CAVs and human-driven vehicles (HVs) coexist. Many recent research works, therefore, have addressed mixed-autonomy traffic where only a portion of the vehicles are CAVs (Cui et al., 2017; Jovanović and Dhingra, 2016; Zheng et al., 2020; Wang et al., 2020, 2022a; Wu et al., 2022; Zhu and Zhang, 2018; Stern et al., 2018). In particular, some of these works have been focusing on how CAVs can influence the overall traffic. In Cui et al. (2017) a single automated vehicle was used to stabilize the traffic flow. The ability of CAVs to dampen stop-and-go waves in mixed traffic was also demonstrated by experiments in Ge et al. (2018) and Stern et al. (2018) and by theoretical analysis in Huang et al. (2020), Li et al. (2014), Yu et al. (2018) and Avedisov et al. (2022). The controllability and reachability of mixed-autonomy traffic were studied by Zheng et al. (2020), which proved that a single CAV can stabilize traffic in the ring-road setting.

In this work, we rely on a specific traffic control strategy by CAVs, that was proposed as *connected traffic control (CTC)* in Molnár et al. (2020) and Molnár et al. (2023) and as *leading cruise control (LCC)* in Wang et al. (2022a) and Wang et al. (2022c). Both of these approaches control the CAV such that it simultaneously adapts its motion to follow the preceding HVs and to lead the following HVs—ultimately allowing the mitigation of traffic oscillations. While these approaches provide the desired string stable behavior, they lack formal guarantees about maintaining safe distances between the vehicles, which our present work seeks to address.

1.2. Safety of mixed-autonomy traffic

Safety is of paramount importance for traffic systems. Although many studies address the potential improvement of efficiency (Talebpour and Mahmassani, 2016; Milanés et al., 2013; Shang and Stern, 2021; Kesting et al., 2010), energy-saving (Vahidi and Sciarretta, 2018; Rios-Torres and Malikopoulos, 2018) and stability (Cui et al., 2017; Zheng et al., 2020; Wang et al., 2020) of the mixed traffic by adopting CAVs, only a few existing works have attempted to evaluate the impact of CAVs on traffic safety. These works include studies about safety under different CAV penetration rates (Ye and Yamamoto, 2019; Li et al., 2017a; Rahman and Abdel-Aty, 2018) and in signalized intersections (Morando et al., 2018; Arvin et al., 2020).

The traffic safety is usually guaranteed by reducing the risk of rear-end collisions. Therefore, a number of safety indicators, also known as surrogate safety measures, have appeared to evaluate the rear-end collision risk by establishing the relationship between the longitudinal safety and car-following state (Vogel, 2003; Li et al., 2017a; Rahman and Abdel-Aty, 2018). Some of these safety measures are *time-based indicators*, such as time headway (TH) and time to collision (TTC), which are constructed based on the time that elapses before a collision could occur (Vogel, 2003). Others measures are *distance-based indicators*, such as distance headway (DH) and minimum stopping distance headway (SDH), which evaluate safety based on the spacing gap between the vehicles (Treiber and Kesting, 2013; Ro et al., 2020). These metrics are essential to construct safety-critical longitudinal controllers for CAVs.

Safety-critical control is usually approached by constraint-handling control methods such as classical optimal control, model predictive control, barrier Lyapunov function (BLF) (Zhu and Zhu, 2019) and control barrier function (CBF) (Ames et al., 2019; Krstic, 2021; Almubarak et al., 2021; Xiao and Belta, 2022). In this work, we rely on the framework of CBFs to maintain safety, due to its ability to take advantage of existing nominal controllers such as those that stabilize traffic. Importantly, CBFs have been applied on a wide range of safety-critical systems, including adaptive cruise control (Ames et al., 2014) and its experimental implementation on heavy-duty trucks (Alan et al., 2022), automated vehicle experiments in multi-lane traffic (Gunter et al., 2022), obstacle avoidance with automated vehicles (Chen et al., 2018), multi-agent systems representing automated vehicles (Jankovic et al., 2022), traffic merging (Xiao et al., 2019), and roundabout crossing (Abduljabbar et al., 2021).

Although the stabilization of traffic by CAVs and the safety-critical control of CAVs have been studied separately in the literature, the integration of these two have not yet been accomplished, to the best of our knowledge. Some works have conducted analysis in this area, such as Li (2022) that quantified the trade-off between stability and safety, and Shi and Li (2021), Makridis et al. (2019) and Gunter et al. (2019) that pointed out that CAVs usually leave comparable or even longer headway than HVs for safety concerns. Our present work intends to fill this gap, via proposing safety-critical traffic control by CAVs. Specifically, a stabilizing nominal traffic controller is adopted, from which a safety-critical controller is synthesized for CAVs with minimum deviation from the nominal controller.

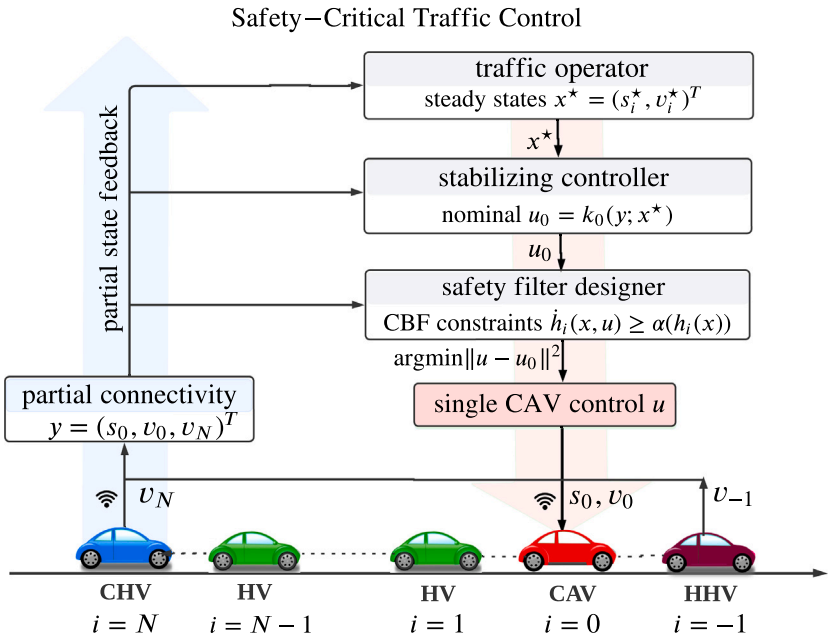

Fig. 1. The proposed *safety-critical traffic control (STC)* framework, wherein mixed traffic is maintained safe by controlling a connected automated vehicle (CAV) amongst human-driven vehicles (HVs) while leveraging vehicle-to-vehicle connectivity with at least one connected human-driven vehicle (CHV) behind the CAV. The STC framework has a hierarchical structure with a *traffic operator* at the top, that can be used to design the desired steady state of the traffic flow, a nominal *stabilizing controller* in the middle, that drives the CAV to mitigate traffic congestion without considering safety, and a *safety filter* at the bottom, that modifies the nominal control input to establish formal safety guarantees for collision avoidance between vehicles.

1.3. Contributions

This paper focuses on providing safety guarantees for mixed-autonomy traffic, which is still an open problem in the literature. In particular, we consider safety-critical control of mixed-autonomy traffic by regulating the motion of a CAV that responds to both preceding and following vehicles. We study the case where a single CAV seeks to stabilize the motion of a vehicle chain behind it by the help of connectivity with at least one human-driven vehicle behind the CAV, while also maintaining guaranteed safety. In our previous work (Zhou and Yu, 2022), we have made an initial step towards this goal, and this paper extends that research by addressing the fact the CAV may not have access to the states of all neighboring vehicles (i.e., it relies on partial state feedback), and by analyzing the underlying performance in more detail. The main contribution of this paper is that we propose a *safety-critical traffic control (STC)* strategy, which provides guaranteed safety for both the CAV and following vehicles, in the cases of full and partial state feedback.

The proposed STC framework is illustrated in Fig. 1 for single-lane mixed traffic including a CAV and several HVs. We control the CAV by assuming that: (I) the CAV detects the head human-driven vehicle (HHV) by on-board range sensors; and (II) at least one of the following HVs is a connected human-driven vehicle (CHV) which the CAV communicates with. That is, the CAV measures its own speed v_0, its spacing s_0, and the speed v_{-1} of the HHV, while connectivity provides access for the CAV to the speed v_N of the CHV. At the same time, the HVs between the CAV and the CHV may not be detected, their states (speeds v_i and spacings s_i) may be unknown to the CAV, but these can be observed by using the data from connectivity. This traffic state information is used in a three-layer hierarchical control structure. In the top layer, a *traffic operator* can be used to command the desired steady states (spacing and velocity) for the mixed traffic. These desired states can be taken from the states of head vehicles, or be calibrated using historical states, or be given from a high-level macroscopic traffic management system (Yu and Krstic, 2019). In the middle layer, a nominal *stabilizing controller* regulates the motion of the CAV in order to drive the traffic towards the desired steady states and fulfill the operator's command, in a string stable fashion. In the bottom layer, a *safety filter* modifies the nominal stabilizing control input using control barrier functions (CBFs) to guarantee safety, and then outputs the final safety-critical controller for the CAV. This framework not only enables flexibility to choose different designs at each layer, but also provides privacy by keeping the details of each design to its own layer only.

The rest of this paper mainly focuses on the safety-critical bottom control layer. The STC framework is established and verified through the following contributions.

- A quadratic program-based controller is constructed to synthesize a safety-critical control input for the CAV. Using this controller, safety guarantees are provided both for the CAV as a hard constraint and for the following HVs as soft constraints. These guarantees are based on various safety measures (TH, TTC and SDH) that are analyzed and compared.

- STC is further extended to the case of output feedback with the help of state observers, to address scenarios in which the CAV does not have access to the states of all the HVs but only to the state of at least one CHV. A state-observer is designed, and a robust CBF is derived to guarantee safety even with inaccurate state estimation.
- Extensive numerical simulations are conducted to show the benefits of the proposed STC, identify its limitations, and analyze the effect of parameters. The simulations also incorporate real trajectory data for the head HV.

The rest of this paper is organized as follows. Section 2 presents the modeling of mixed-autonomy traffic, and revisits a nominal control approach for CAVs to stabilize traffic. Section 3 introduces the framework of STC, to modify the nominal controller and endow it with formal safety-guarantees. To this end, safe spacing policies are described, the theory of control barrier functions is revisited, and state observers are utilized in case of output feedback. Section 4 provides extensive numerical simulations (that involve vehicle trajectories from real data) to demonstrate the efficacy of STC. Section 5 concludes the paper.

2. Smoothing mixed-autonomy traffic by connected automated vehicles

We first model the longitudinal dynamics of mixed-autonomy traffic. We consider a single-lane scenario that involves a head vehicle (HHV), followed by a single connected automated vehicle (CAV) and N subsequent human-driven vehicles (HVs); see Fig. 1. We revisit the notion of string stability and design a nominal controller for the CAV that can stabilize the traffic behind it. We first consider that all HVs are connected to the CAV, then address the case of partial connectivity with a single connected human-driven vehicle (CHV). This controller will be endowed with provable safety guarantees in the next section.

2.1. Modeling of mixed-autonomy traffic

The mixed-autonomy traffic model constitutes two parts: a car-following model for HVs and a model for the longitudinal control of the CAV. The car-following dynamics of the HVs (indexed $i \in \{1, \dots, N\}$) are described as

$$\begin{aligned} \dot{s}_i &= v_{i-1} - v_i, \\ \dot{v}_i &= F_i\left(s_i, \dot{s}_i, v_i\right), \end{aligned} \tag{1}$$

where $s_i \in \mathbb{R}$ represents the spacing (distance headway) between HV i and its predecessor vehicle $i-1$. Function $F_i : \mathbb{R}^3 \to \mathbb{R}$ describes how HV i controls its acceleration for car-following as a function of its own velocity $v_i \in \mathbb{R}$, the spacing s_i and the derivative $\dot{s}_i \in \mathbb{R}$ of the spacing (i.e., the relative speed). For the CAV (with index $i = 0$), the longitudinal dynamics are governed by

$$\begin{aligned} \dot{s}_0 &= v_{-1} - v_0, \\ \dot{v}_0 &= u, \end{aligned} \tag{2}$$

where the acceleration of the CAV is the control input $u \in \mathbb{R}$ to be designed, and $v_{-1} \in \mathbb{R}$ is the velocity of the HHV ($i = -1$).

The state of the mixed-autonomy traffic model (1)–(2) is $n = 2N + 2$ dimensional, and it consists of the spacing and speed of the CAV and the following HVs, given by $x \in \mathbb{R}^n$,

$$x = \begin{bmatrix} s_0 & v_0 & \dots & s_N & v_N \end{bmatrix}^\top. \tag{3}$$

This leads to a general nonlinear mixed-autonomy traffic model

$$\dot{x} = f(x, r) + g(x)u, \tag{4}$$

$$f(x,r) = \begin{bmatrix} f_0(x,r) \\ f_1(x) \\ \vdots \\ f_N(x) \end{bmatrix}, \quad g(x) = \begin{bmatrix} g_0 \\ 0_{2\times 1} \\ \vdots \\ 0_{2\times 1} \end{bmatrix}, \quad f_0(x,r) = \begin{bmatrix} v_{-1} - v_0 \\ 0 \end{bmatrix}, \quad f_i(x) = \begin{bmatrix} v_{i-1} - v_i \\ F_i(s_i, v_{i-1} - v_i, v_i) \end{bmatrix}, \quad g_0 = \begin{bmatrix} 0 \\ 1 \end{bmatrix}, \tag{5}$$

where $r = v_{-1}$ is a time-varying reference signal, $0_{2\times 1}$ is the two dimensional zero vector, and $f : \mathbb{R}^n \times \mathbb{R} \to \mathbb{R}^n$, $g : \mathbb{R}^n \to \mathbb{R}^n$. Note that, alternatively, one could also formulate this model using the longitudinal positions p_i of the vehicles' rear bumper, that are related to the spacings s_i through the vehicle lengths l_i as $s_i = p_{i-1} - p_i - l_i$.

For simplicity, we design a nominal controller for the CAV based on linearization of the dynamics. Thus, we first consider the steady state of the system, given by the equilibrium speed $v^\star$ as $v_i(t) \equiv v^\star$ and the equilibrium spacing $s_i^\star$ as $s_i(t) \equiv s_i^\star$, $i \in \{0, \dots, N\}$. Note that the equilibrium spacing $s_i^\star$ of the HVs ($i \in \{1, \dots, N\}$) satisfy

$$F_i\left(s_i^\star, 0, v^\star\right) = 0, \tag{6}$$

and these may be different from the equilibrium spacing $s_0^\star$ of the CAV that is determined by its controller. The equilibrium speed v^* could be designed by government policy or macroscopic control policies that optimize the whole traffic flow (Yu and Krstic, 2019); cf. Fig. 1. Without external guidance of a desired v^*, we can take the head vehicle's constant speed as equilibrium speed v^* so that the following vehicles will drive at the same speed.

Using the perturbations $\tilde{s}_i = s_i - s_i^\star$ and $\tilde{v}_i = v_i - v^\star$, the linearized dynamics can be obtained from (1)–(2) as

$$\begin{aligned} \dot{\tilde{s}}_i &= \tilde{v}_{i-1} - \tilde{v}_i, \\ \dot{\tilde{v}}_i &= a_{i1}\tilde{s}_i - a_{i2}\tilde{v}_i + a_{i3}\tilde{v}_{i-1}, \end{aligned} \tag{7}$$

where $a_{i1} = \frac{\partial F_i}{\partial s_i}, a_{i2} = \frac{\partial F_i}{\partial \dot{s}_i} - \frac{\partial F_i}{\partial v_i}, a_{i3} = \frac{\partial F}{\partial \dot{s}_i}$ are evaluated at the steady states, and

$$\begin{aligned} \dot{\tilde{s}}_0 &= \tilde{v}_{-1} - \tilde{v}_0, \\ \dot{\tilde{v}}_0 &= u. \end{aligned} \tag{8}$$

The state of the linearized mixed-autonomy traffic model is

$$x = \begin{bmatrix} \tilde{s}_0 & \tilde{v}_0 & \dots & \tilde{s}_N & \tilde{v}_N \end{bmatrix}^\top, \tag{9}$$

hence (7)–(8) can be written in the compact form

$$\dot{x} = Ax + Bu + Dr, \tag{10}$$

$$A = \begin{bmatrix} P_0 & & & & \\ Q_1 & P_1 & & & \\ & \ddots & \ddots & & \\ & & Q_N & P_N \end{bmatrix}, \ B = \begin{bmatrix} b_0 \\ 0_{2\times 1} \\ \vdots \\ 0_{2\times 1} \end{bmatrix}, \ D = \begin{bmatrix} d_0 \\ 0_{2\times 1} \\ \vdots \\ 0_{2\times 1} \end{bmatrix}, \ P_0 = \begin{bmatrix} 0 & -1 \\ 0 & 0 \end{bmatrix}, \ P_i = \begin{bmatrix} 0 & -1 \\ a_{i1} & -a_{i2} \end{bmatrix}, \ Q_i = \begin{bmatrix} 0 & 1 \\ 0 & a_{i3} \end{bmatrix}, \ b_0 = \begin{bmatrix} 0 \\ 1 \end{bmatrix}, \ d_0 = \begin{bmatrix} 1 \\ 0 \end{bmatrix}, \tag{11}$$

where $r = \tilde{v}_{-1}$ and $A \in \mathbb{R}^{n\times n}$, $B, D \in \mathbb{R}^n$. We use the same notation x for the state of the nonlinear system (4) and the linear one (10) to emphasize that the proposed STC works for both of these two system formulations.

The models (4) and (10) describe mixed-autonomy traffic for the general case where the CAV can detect both the preceding vehicle and the following vehicles. In application, there could also occur two special cases where the CAV is at the head or the tail of the vehicle chain. If the CAV is the head vehicle (i.e., there is no HHV ahead of it, or it is far enough to be ignored), then we can still formulate the system with $f_0(x, r) = 0_{2\times 1}$ or $d_0 = 0_{2\times 1}$. If the CAV is at the tail of the vehicle chain (i.e., there are no connected follower HVs), then the model applies with the state $x = \begin{bmatrix} \tilde{s}_0 & \tilde{v}_0 \end{bmatrix}^\top$.

In this paper, we focus on the longitudinal control of the CAV. The lateral dynamics of the CAV, or those of potential cutting-in vehicles during the lane-changing process, are out of the scope of this paper, although our work could be integrated with lateral controllers to enhance safety (Monteiro and Ioannou, 2023). For example, if a vehicle cut into the lane between the CAV and the HHV, then our model would only consider this event by setting this vehicle as the new HHV after the cut-in.

2.2. Nominal controller design and head-to-tail string stability

Now we design a nominal control input u_0 that allows the CAV to follow the head vehicle while leading N HVs such that the resulting traffic flow is smooth—specifically, *string stable*. In the next section, we modify u_0 to an input u that also has formal safety guarantees for collision avoidance (without restriction on the choice of the nominal controller u_0).

Connectivity allows the CAV to obtain the speeds v_i and positions p_i of the HVs based on GPS and basic safety messages. This information characterizes the state of the human-driven traffic behind the CAV, hence the CAV may use these data to control and stabilize the traffic flow, ultimately mitigating traffic congestions. This led to the idea of *connected traffic control (CTC)* in Molnár et al. (2020) and Molnár et al. (2023), where the CAV responds to the state v_i, p_i of the HVs (obtained from connectivity) while considering the state v_{-1}, p_{-1} of the head vehicle (provided by range sensors or connectivity), using a control law of the form

$$u_0 = \bar{F}_0(p_{-1}, v_{-1}, p_0, v_0, p_1, v_1, \dots, p_N, v_N). \tag{12}$$

Note that if the CAV is not connected to an HV and does not have access to its state, the corresponding state p_i, v_i is omitted from the response. Examples for CTC (12) and their analysis in the presence of response delays can be found in Molnár et al. (2023).

In special cases, the positions p_i can be converted into the spacings s_i, resulting in a controller:

$$u_0 = F_0(v_{-1}, s_0, v_0, s_1, v_1, \dots, s_N, v_N). \tag{13}$$

This conversion requires that all longitudinal positions p_i and vehicle lengths are known to the CAV or, alternatively, CHVs could also potentially communicate their spacing (i.e., realize cooperative perception). Furthermore, if the CAV even has access to the perturbations $\tilde{s}_i$, $\tilde{v}_i$ (not just s_i, v_i), then a linear controller can be formulated as

$$u_0 = a_1\tilde{s}_0 - a_2\tilde{v}_0 + a_3\tilde{v}_{-1} + \sum_{i=1}^{N} \left(\mu_i\tilde{s}_i + k_i\tilde{v}_i\right), \tag{14}$$

where μ_i, k_i are the feedback gains corresponding to the state of vehicle i. These gains can be designed based on the linear model (10). Controller (14) is called *leading cruise control (LCC)*, and it was proposed in Wang et al. (2022a).

The above traffic control strategies can be compactly written as

$$u_0 = k_0(x, r), \tag{15}$$

where the state x and reference signal r can be associated either with the nonlinear model (4) or with the linear model (10). For simplicity, the examples of this paper are presented for the linear model (10) and the linear LCC strategy (14) as nominal controller, under the assumption that the parameters of the HVs are identical: $a_{i1} = a_1$, $a_{i2} = a_2$, $a_{i3} = a_3$, $\forall i \in \{1, \dots, N\}$. The general framework of STC, however, could accommodate any other nominal stabilizing controller of the form (15).

In order to design the gains μ_i, k_i of the nominal controller (14), first we notice that the pair (A, B) is controllable for $a_1 - a_2 a_3 + a_3^2 \neq 0$, which was proven in Wang et al. (2022a). Under this condition, we can design the control gains such that speed perturbations decay along the chain of vehicles and traffic congestions are mitigated, i.e., the closed-loop system is *string stable*. While there exist various definitions of string stability (Feng et al., 2019), suited both for nonlinear and linear dynamics, we focus on one particular notion, *head-to-tail string stability* (Zhang and Orosz, 2016), that is convenient for the analysis of linear systems.

Head-to-tail string stability is frequently used to evaluate the CAV's ability to attenuate velocity fluctuations, thereby mitigating congestions, smoothing and stabilizing traffic. Given the Laplace transforms $\tilde{V}_{-1}(s)$, $\tilde{V}_N(s)$ of the velocity perturbations $\tilde{v}_{-1}(t)$, $\tilde{v}_N(t)$ of the head and tail vehicles, the head-to-tail transfer function (Zhang and Orosz, 2016) is defined as

$$G(s) = \frac{\tilde{V}_N(s)}{\tilde{V}_{-1}(s)}. \tag{16}$$

This function characterizes how much speed perturbations amplify along the mixed chain of $N + 2$ vehicles. Head-to-tail string stability holds if and only if (Zhang and Orosz, 2016)

$$|G(\mathrm{j}\omega)|^2 < 1, \quad \forall \omega > 0, \tag{17}$$

where $\mathrm{j}^2 = -1$. This condition means that the speed fluctuations of the tail vehicle are smaller in steady state than those of the head vehicle for any angular frequency ω.

For the linearized system (10) with controller (14), Wang et al. (2022a) derived the head-to-tail transfer function in the form

$$G(s) = \frac{\phi(s)}{\psi(s) - \sum_{i=1}^{N} \left(\mu_i \left(\frac{\phi(s)}{\psi(s)} - 1 \right) + k_i s \right) \left(\frac{\psi(s)}{\phi(s)} \right)^i} \left(\frac{\phi(s)}{\psi(s)} \right)^N, \tag{18}$$

with

$$\phi(s) = a_3 s + a_1, \quad \psi(s) = s^2 + a_2 s + a_1. \tag{19}$$

This expression enables one to design μ_i and k_i such that (17) holds and head-to-tail string stability is attained; see Wang et al. (2022a).

2.3. Observer design

Notice that controllers of the form (15) rely on the full state x of the system. As stated in Wang et al. (2022b), however, it may be difficult to measure all state variables in x. Instead, an output $y \in \mathbb{R}^{n_y}$ may be available, given by a function $c : \mathbb{R}^n \to \mathbb{R}^{n_y}$ of the state:

$$y = c(x). \tag{20}$$

This is also the case when some of the HVs are not equipped with communication devices and their speeds and gaps are unavailable to the CAV. Then, we have the output as

$$y = Cx, \tag{21}$$

with $C \in \mathbb{R}^{n_y \times n}$ being the observation matrix. For example, if only vehicle N is a CHV, like in Fig. 1, then the CAV can only have access to the velocity v_N and its own state s_0 and v_0, or the corresponding perturbations $\tilde{v}_N$, $\tilde{s}_0$ and $\tilde{v}_0$. This leads to

$$y = \begin{bmatrix} \tilde{s}_0 & \tilde{v}_0 & \tilde{v}_N \end{bmatrix}^\top, \tag{22}$$

and the observation matrix

$$C = \begin{bmatrix} 1 & 0 & \cdots & & & 0 \\ 0 & 1 & 0 & \cdots & & 0 \\ 0 & & & \cdots & 0 & 1 \end{bmatrix}. \tag{23}$$

In order to overcome that only the output y is available instead of the full state x, we use state observers to establish an estimate $\hat{x}$ of the state using the output. This requires the state of the system to be observable. The observability of the linear mixed-autonomy traffic model (10) is discussed in Wang et al. (2022a), where it is shown that the CAV needs access to at least $\tilde{s}_0$, $\tilde{v}_0$ and $\tilde{v}_N$ in order for the state of the vehicle chain between the CAV and the CHV to be observable. This is the minimum information required to design an observer. Both for linear and nonlinear dynamics, state observers are usually constructed as dynamical systems that

describe the evolution of the estimated state $\hat{x}$ with corresponding estimated output $\hat{y} = \tilde{c}(\hat{x})$. For example, control-affine observers are of the form

$$\dot{\hat{x}} = \tilde{f}(\hat{x}, r, y) + \tilde{g}(\hat{x}, r, y)u \tag{24}$$

where the dynamics $\tilde{f}$, $\tilde{g}$ are designed so that $\hat{x}$ converges to the true state x. That is, the observer estimation error

$$e = \hat{x} - x \tag{25}$$

needs to converge to zero with time.

For simplicity, we focus on observing the internal states of the linear model (10) using the linear output (21). First, we notice that the pair (A, C) is observable for $a_1 - a_2 a_3 + a_3^2 \neq 0$, which was proven in Wang et al. (2022a). Under this condition, we design a Luenberger observer (Luenberger, 1971; Callier and Desoer, 2012):

$$\dot{\hat{x}} = A\hat{x} + Bu + L(y - \hat{y}) + Dr, \tag{26}$$

where $\hat{y} = C\hat{x}$, $\tilde{f}(\hat{x}, r, y) = A\hat{x} + Dr + L(y - \hat{y})$, $\tilde{g}(\hat{x}, r, y) = B$, while $L \in \mathbb{R}^{n \times n_y}$ is the constant observer gain to be designed. Thus, we express the time derivative of (25) as

$$\dot{e} = (A - LC)e, \tag{27}$$

where L is chosen using pole placement so that matrix $A - LC$ is Hurwitz and the error dynamics (27) are exponentially stable. Considering measurement noise and unmodeled dynamics, as a rule-of-thumb, the observer gain L is preferably chosen so that the real parts of the eigenvalues of $A - LC$ are not extremely low or high values.

With a well-designed observer, the error is bounded as follows:

$$\|e(t)\| \leq M(t), \quad \forall t \geq 0, \tag{28}$$

where $\|.\|$ is Eucledian norm, while $M(t) \geq 0$ is a known time-varying function whose values are non-negative and that depends on x_0, $\hat{x}_0$. Specifically, for the Luenberger observer (26) we have the bound

$$\|e(t)\| \leq M_0 \mathrm{e}^{-\lambda t}, \quad \forall t \geq 0, \tag{29}$$

where $M_0 \geq 0$ depends on $e_0 = \hat{x}_0 - x_0$, whereas $\lambda > 0$ is associated with the real part of the rightmost eigenvalue of $A - LC$. Note that one could also design observers of the form (24) for the nonlinear system (4) with the general output (20), such that they satisfy (28) with some $M(t)$; see for example Wang and Xu (2022). However, nonlinear observer design is out of scope of this paper, and instead we focus on safety-critical control.

3. Safety-critical traffic control by connected automated vehicles

While a well-designed controller of form (15) may achieve string stable behavior for the mixed vehicle chain, it may not guarantee that vehicles maintain safe distances between each other. Naïve stabilization of the mixed traffic could lead to unsafe driving conditions for individual vehicles. Therefore, now we propose the strategy of *safety-critical traffic control (STC)*, in which we synthesize a safety-critical controller for the CAV using control barrier functions and a nominal input that stabilizes traffic. First, two main safety requirements are identified, and various safe spacing policies are discussed. Then, control barrier functions are used to endow the controlled traffic system with safety for a wide range of nominal controllers. Finally, the case of output feedback is addressed. The end result is formal safety guarantees for the mixed-autonomy traffic.

3.1. Safety requirements and safe spacing policies

We address two main requirements that are needed to avoid safety-critical failures for the STC system. The first requirement is the *CAV's safety*. This means that the CAV ($i = 0$) maintains a safe distance to the head vehicle ($i = -1$), i.e., specific constraints on the spacing $s_0(t)$ must be satisfied for all time, regardless of the HVs' driving behavior. This guarantees the avoidance of collision between the CAV and the head vehicle, including situations, for example, when the head vehicle brakes abruptly due to an unexpected cut-in vehicle or crossing pedestrians. The second requirement is the *HVs' safety*. This means that all of the N HVs ($i \in \{1, \ldots, N\}$) behind the CAV maintain safe distances, i.e., $s_i(t)$ satisfy safety constraints provided that the HVs drive according to a selected car-following model. Importantly, while the HVs' safety primarily depends on their own driving behavior, it is possible to enhance their safety by controlling the CAV. For example, if the CAV makes an unnecessarily harsh brake for its own safety, it could cause a collision in the following chain of HVs, but this can be avoided by taking into account the HVs' safety in the CAV's controller design. Similarly, the CAV can also accelerate (if it is safe to do so) to make space for the following HVs and help avoid a collision between them. That is, STC seeks to make the CAV's driving behavior both safe and considerate of the traffic behind it, to avoid collisions for both the CAV and the HVs.

To satisfy these requirements, we provide a set of *safe spacing policies* that constrain the spacings s_i ahead of the CAV and HVs. The *time headway (TH)* policy guarantees a minimum constant time headway $\tau > 0$ based on the spacing and speed:

$$s_i \geq \tau v_i. \tag{30}$$

Similarly, the *time-to-collision (TTC)* policy maintains a minimum time-to-collision $\tau > 0$ based on the relative speed:

$$s_i \geq \tau(v_i - v_{i-1}). \tag{31}$$

The *stopping distance headway (SDH)* policy guarantees a minimum stopping distance while incorporating the follower vehicle's braking limit $a_{i,\min}$ in addition to the time-to-collision (Treiber and Kesting, 2013):

$$s_i \geq \tau(v_i - v_{i-1}) + \frac{(v_i - v_{i-1})^2}{2|a_{i,\min}|}. \tag{32}$$

Finally, the *distance headway (DH)* policy guarantees a minimum constant spacing $s_{i,\min}$ between vehicles: $s_i \geq s_{i,\min}$. However, this choice disregards the speed of the vehicles, hence we rather focus on the first three spacing policies. Similarly, for the linearized system (10), we can write the safe spacing policies as

$$\tilde{s}_i \geq \tau(\tilde{v}_i + v^\star) - s_i^\star, \tag{33}$$

$$\tilde{s}_i \geq \tau(\tilde{v}_i - \tilde{v}_{i-1}) - s_i^\star, \tag{34}$$

$$\tilde{s}_i \geq \tau(\tilde{v}_i - \tilde{v}_{i-1}) + \frac{(\tilde{v}_i - \tilde{v}_{i-1})^2}{2|a_{i,\min}|} - s_i^\star. \tag{35}$$

Next, we will introduce control barrier functions to guarantee the satisfaction of these safe spacing policies in the closed-loop system. Furthermore, we will compare the effectiveness of these policies in safety enforcement in mixed traffic control.

The above safe spacing criteria can be stated equivalently as $x \in C_i$, i.e., the state x remains inside a safe set C_i, given by

$$C_i = \left\{ x \in \mathbb{R}^n : h_i(x) \geq 0 \right\}, \tag{36}$$

where the different candidates for function $h_i(x)$ are defined by

$$h_i^{\mathrm{TH}}(x) = s_i - \tau v_i, \tag{37}$$

$$h_i^{\mathrm{TTC}}(x) = s_i - \tau(v_i - v_{i-1}), \tag{38}$$

$$h_i^{\mathrm{SDH}}(x) = s_i - \tau(v_i - v_{i-1}) - \frac{(v_i - v_{i-1})^2}{2|a_{i,\min}|}, \tag{39}$$

and by the corresponding expressions with tilde.

In order to maintain safety, we seek to achieve that if the traffic system is safe initially, then the CAV's controller prevents safety violations for all time. That is, for any initial condition $x_0 \in C_i$ the state of the closed-loop system must satisfy $x(t) \in C_i$ for all $t \geq 0$ and for all $i \in \{0, \dots, N\}$. In other words, the controller must render the set $C = \bigcap_{i=0}^{N} C_i$ forward invariant under the closed-loop dynamics. We achieve this goal by using control barrier functions.

3.2. Guaranteed safety via control barrier functions and quadratic programs

To design a safety-critical controller, we revisit the theory of control barrier functions. We consider affine control systems:

$$\dot{x} = f(x, r) + g(x)u, \tag{40}$$

where $x \in \mathbb{R}^n$, $r \in \mathbb{R}^l$ and $u \in \mathbb{R}^m$, while $f : \mathbb{R}^n \times \mathbb{R}^l \to \mathbb{R}^n$ and $g : \mathbb{R}^n \to \mathbb{R}^{n \times m}$ are locally Lipschitz continuous. This may represent the nonlinear mixed traffic system (4), or the linear system (10) by the substitution $f(x, r) = Ax + Dr$, $g(x) = B$. We seek to keep the state x inside a safe set $C \subset \mathbb{R}^n$, that is defined by a continuously differentiable function $h : \mathbb{R}^n \to \mathbb{R}$ as

$$C = \{ x \in \mathbb{R}^n : h(x) \geq 0 \}, \tag{41}$$

cf. (36), where h satisfies $h(x) = 0 \implies \frac{\partial h}{\partial x}(x) \neq 0$. We achieve this goal via control barrier functions.

Definition 1 (*Control Barrier Function Ames et al. (2014)*). Function h is a *control barrier function (CBF)* for system (40) if there exists an extended class-$\mathcal{K}_\infty$ function[1] α such that for all $x \in \mathbb{R}^n$:

$$\sup_{u \in \mathbb{R}^m} \Big[\underbrace{L_f h(x, r) + L_g h(x) u}_{\dot{h}(x, r, u)} \Big] > -\alpha(h(x)), \tag{42}$$

where $L_f h(x, r) = \frac{\partial h}{\partial x}(x) f(x, r)$ and $L_g h(x) = \frac{\partial h}{\partial x}(x) g(x)$.

The expression in (42) inside the brackets is the first time derivative of h along the system (40). Note that condition (42) sufficiently holds if $L_g h(x) \neq 0$ for all $x \in \mathbb{R}^n$. In such a case, the first derivative of h is affected by the input u regardless of the state x—this is termed as h has *relative degree one*. Given a CBF, the following result on safety was established by Ames et al. (2014).

[1] A continuous function $\alpha : \mathbb{R} \to \mathbb{R}$ belongs to extended class-$\mathcal{K}_\infty$ if it is strictly monotonically increasing, $\alpha(0) = 0$ and $\lim_{r \to \pm\infty} \alpha(r) = \pm\infty$.

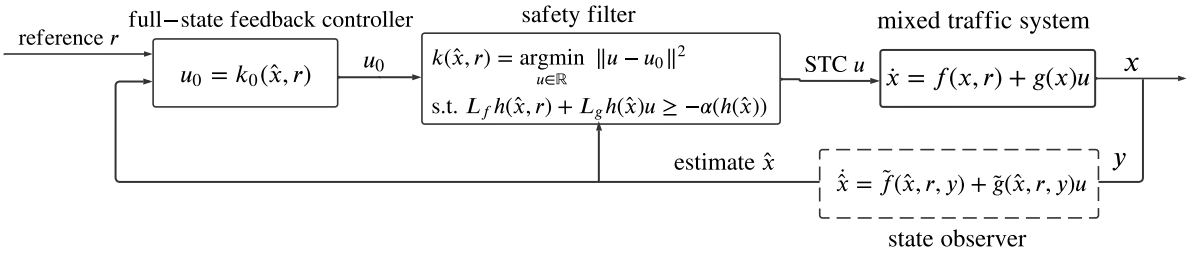

Fig. 2. Block diagram of full-state feedback safety-critical traffic control (STC) and observer-based output feedback STC. STC modifies a nominal controller—that stabilizes mixed traffic but is not necessarily safe—to a safety-critical controller by using a safety filter that includes control barrier functions (CBFs). The dashed block represent the observer design for state estimation. This block can be omitted in case of full state feedback but is included in case of output feedback.

Theorem 1 (*Guaranteed Safety Via CBF Ames et al. (2014)*). *If h is a CBF for system (40), then any locally Lipschitz continuous controller $k : \mathbb{R}^n \times \mathbb{R}^l \to \mathbb{R}$, $u = k(x, r)$, that satisfies*

$$L_f h(x, r) + L_g h(x)u \geq -\alpha(h(x)), \tag{43}$$

renders the set C in (41) forward invariant (safe) under the closed-loop dynamics, such that $x_0 \in C \implies x(t) \in C$, $\forall t \geq 0$.

As such, controllers that satisfy (43) provide provable safety guarantees, while condition (42) ensures that such controllers exist. We use (43) for safety-critical control design. Suppose that there exists a feedback controller, $u_0 = k_0(x, r)$, that is stabilizing but may not necessarily be safe. Then, the input u_0 can be modified in a minimally invasive fashion to an input u that satisfies (43) by using the following quadratic program (QP) based controller design (Ames et al., 2019):

$$\begin{aligned} k(x, r) = \underset{u\in\mathbb{R}}{\operatorname{argmin}}\ & \|u - u_0\|^2 \\ \text{s.t. } & L_f h(x, r) + L_g h(x)u \geq -\alpha(h(x)). \end{aligned} \tag{44}$$

Controller $u = k(x, r)$ is safety-critical, and ensures safety with minimum deviation from the nominal controller $u_0 = k_0(x, r)$. Note that (44) is often called as *safety filter*. The role of the safety filter in STC is illustrated in Fig. 2 and discussed next.

3.3. Safety-critical traffic control

Now we implement CBFs on the mixed traffic system and synthesize a STC strategy via a quadratic program. Specifically, we rely on the CBF candidates h_i in (37)–(39). To apply the CBF theory, however, first we must show that these candidates are indeed CBFs and satisfy (42). To investigate condition (42), we consider the TH policy (37) as example, although the conclusions below hold for the other spacing policies in (38)–(39), too. Function h_0, that is associated with the CAV's safety, satisfies $L_g h_0(x) = -\tau \neq 0$. Hence it has relative degree one and it is a valid CBF that satisfies (42). This results from the fact that the CAV's safety is directly affected by the CAV's control input. However, the remaining functions h_i ($i \in \{1, \dots, N\}$) are associated with the HVs' safety, and they are not directly affected by the CAV's controller. Instead, $L_g h_i(x) = 0$ and (42) does not hold for all $x \in \mathbb{R}^n$, hence h_i are not valid CBFs. In fact, the control input u shows up in the $(i+1)$-st time derivative of h_i, making it relative degree $i+1$. Although there exist more complex control designs for high relative degree scenarios (Nguyen and Sreenath, 2016; Ames et al., 2019), we seek to avoid this complexity, especially since the relative degree of h_i depends on the number of vehicles.

Instead, we propose to construct CBFs with a novel method that is compatible with all safe spacing policies. Specifically, we modify the CBF candidates h_i to

$$\bar{h}_i(x) = h_i(x) - h_0(x), \tag{45}$$

that have relative degree one irrespective of the number of vehicles. It should be noted that $\bar{h}_i(x) \geq 0$ and $h_0(x) \geq 0$ are sufficient conditions for $h_i(x) \geq 0$. Thus, $\bar{h}_i$ are valid CBFs that allow the satisfaction of the safe spacing policies given by h_i.

The CBFs h_0 and $\bar{h}_i$ lead to the following constraints on u to satisfy the requirements of the CAV's safety and HVs' safety. The constraint that guarantees safe spacing between the head vehicle and the CAV becomes

$$L_f h_0(x, r) + L_g h_0(x)u + \gamma_0 h_0(x) \geq 0, \tag{46}$$

where, for simplicity, we chose the extended class-$\mathcal{K}_\infty$ function α in (43) to be linear, i.e., $\alpha(h_0) = \gamma_0 h_0$ with a tunable constant $\gamma_0 > 0$. Parameter γ_0 balances the trade-off between safety, driving comfort and conservativeness. With a smaller γ_0, the CAV typically has a less abrupt accelerations, but this choice could also result in a more conservative driving behavior. Similarly, the constraints that yield safe spacings ahead of the HVs are given by

$$L_f \bar{h}_i(x, r) + L_g \bar{h}_i(x)u + \gamma_i \bar{h}_i(x) + \sigma_i \geq 0, \tag{47}$$

where $\gamma_i > 0$, $i \in \{1, \dots, N\}$, while the role of $\sigma_i \geq 0$ is explained below. In (46)–(47), the functions f and g can be either from the nonlinear system (4) or the linear system (10), and a corresponding safety-critical controller can be designed based on either of these models.

We remark that while the CBF condition (42) ensures that there exists a control input u satisfying the safety constraint (43), there is no such existence guarantee if multiple constraints like (46)–(47) are enforced simultaneously. In other words, the CAV's and HVs' safety constraints (46)–(47) may conflict in some scenarios. In such cases, we prioritize the CAV's safety over the HVs' safety by setting the CAV's safety constraint (46) as a hard constraint and the HV's constraints (47) as soft constraints. This approach can be justified from four aspects: (I) the CAV's controller is primarily responsible for its own safety; (II) if a collision happened at the CAV, the following HVs would also be affected; (III) in practice, the HVs do not necessarily drive according to the selected human driver model; and (IV) if the CAV's safety constraint $h_0(x) \geq 0$ is not satisfied, $\bar{h}_i(x) \geq 0$ no longer implies $h_i(x) \geq 0$, i.e., the HVs' safety may be compromised. Therefore, we resolve the conflict between multiple safety constraints by introducing the relaxation variables σ_i into the HVs' safety constraints. This makes (47) soft constraints while keeping (46) as a hard constraint.

Finally, we incorporate the safety constraints (46)–(47) and the traffic controller (15) that yields string stable behavior into an optimization problem to establish the proposed STC. Specifically, while enforcing (46)–(47), we minimize the deviation of the control input u from the nominal stabilizing input u_0. This leads to the quadratic program (QP):

$$
\begin{aligned}
k(x, r) = \underset{u \in \mathbb{R}, \sigma_i \geq 0}{\operatorname{argmin}} \quad & |u - u_0|^2 + \textstyle\sum_{i=1}^{N} p_i \sigma_i^2 \\
\text{s.t.} \quad & \text{CAV}'\text{s safety}: \quad L_f h_0(x, r) + L_g h_0(x) u + \gamma_0 h_0(x) \geq 0, \\
& \text{HVs}'\text{ safety}: \quad \begin{cases} L_f \bar{h}_1(x, r) + L_g \bar{h}_1(x) u + \gamma_1 \bar{h}_1(x) + \sigma_1 \geq 0, \\ \quad \vdots \\ L_f \bar{h}_N(x, r) + L_g \bar{h}_N(x) u + \gamma_N \bar{h}_N(x) + \sigma_N \geq 0, \end{cases}
\end{aligned}
\tag{48}
$$

cf. (44), where σ_i are the slack variables to relax HVs' safety constraints and ensure the feasibility of the QP, while $p_i \gg 1$ are penalty coefficients. If the solution of the QP is $\sigma_i^* = 0$, then both the CAV's safety constraint (46) and HVs' safety constraint (47) are met. If $\sigma_i^* \neq 0$, then the CAV's safety is prioritized, and the HVs are no longer guaranteed to be safe. Furthermore, when there is a conflict between the safety and string stability of mixed traffic (i.e., u_0 does not satisfy the safety constraints), the QP enforces safety ($u \neq u_0$) and sacrifices string stability at the minimum cost. Finally, we remark that if there were no following HVs connected to the CAV, then a simpler QP with only the CAV's safety constraint (46) could still be constructed from (48) as a special case to drive the CAV with safe adaptive cruise control.

3.4. Safety with observer-based control barrier functions

The proposed STC strategy (15)–(48) relies on full state feedback. In practice, however, some state information may not be available to the CAV. In Section 2.3, we highlighted that this can be overcome by output feedback and state observers if the mixed-autonomy traffic system is observable, i.e., the speed v_N of the CHV is available to the CAV. In this section, we extend the STC design to output feedback where only partial states of HVs are available. We propose to use state observers for state estimation, that allows us to execute safety-critical controllers using an estimate of the unknown states; see Fig. 2. Below we provide a set of simple conditions under which formal safety guarantees are maintained despite observer estimation errors. These results follow the constructions in Agrawal and Panagou (2023), where a comprehensive safety-critical control framework with observers was established. For another approach on the combination of observers and CBFs, please also see Wang and Xu (2022).

Consider an observer (24) that satisfies (28). Let the CBF h have the Lipschitz coefficient $\mathcal{L} > 0$, satisfying:

$$
|h(\hat{x}) - h(x)| \leq \mathcal{L} \|\hat{x} - x\|, \tag{49}
$$

and for simplicity, let the class-$\mathcal{K}$ function α be linear, $\alpha(r) = \gamma r$. Furthermore, consider the set

$$
\hat{C}(t) = \left\{ \hat{x} \in \mathbb{R}^n : \hat{h}(\hat{x}, t) \geq 0 \right\}, \tag{50}
$$

$$
\hat{h}(\hat{x}, t) = h(\hat{x}) - \mathcal{L} M(t), \tag{51}
$$

where $\hat{h}(\hat{x}, t)$ represents the worst-case value of $h(x)$ that may correspond to an estimated state $\hat{x}$ given the estimation error bound $M(t)$. Then, we have the following result on safety.

Theorem 2 (*Guaranteed Safety with Observer Agrawal and Panagou (2023)*). *Consider the system (40), the safe set (41), and an observer (24) that satisfies (28). If h is a CBF for system (24) with Lipschitz coefficient $\mathcal{L}$, then any locally Lipschitz continuous controller $k : \mathbb{R}^n \times \mathbb{R}^l \times \mathbb{R}^{n_y} \to \mathbb{R}$, $u = k(\hat{x}, r, y)$, that satisfies*

$$
L_{\hat{f}} h(\hat{x}, r, y) + L_{\hat{g}} h(\hat{x}, r, y) u \geq -\gamma h(\hat{x}) + \mathcal{L}\left(\dot{M}(t) + \gamma M(t)\right), \tag{52}
$$

renders set $\hat{C}(t)$ in (50)–(51) forward invariant under the closed-loop dynamics, such that $\hat{x}_0 \in \hat{C}(0) \implies \hat{x}(t) \in \hat{C}(t)$, $\forall t \geq 0$. Furthermore, $\hat{x}(t) \in \hat{C}(t) \implies x(t) \in C$ holds, that ultimately leads to safe behavior.

Proof. First, we express the total time derivative of $\hat{h}$ defined in (51) as

$$\dot{\hat{h}}(\hat{x}, t, r, y, u) = L_{\hat{f}} h(\hat{x}, r, y) + L_{\hat{g}} h(\hat{x}, r, y)u - \mathcal{L}\dot{M}(t). \tag{53}$$

With this, (51)–(52) lead to

$$\dot{\hat{h}}(\hat{x}, t, r, y, u) \geq -\gamma \hat{h}(x, t). \tag{54}$$

Therefore, we can apply the time-varying counterpart (Xu, 2018) of Theorem 1 that yields the invariance of $\hat{C}(t)$. Finally, $\hat{x}(t) \in \hat{C}(t) \implies x(t) \in C$ is equivalent to $\hat{h}(\hat{x}(t), t) \geq 0 \implies h(x(t)) \geq 0$, which can be proven by

$$\begin{aligned} \hat{h}(\hat{x}, t) &= h(\hat{x}) - \mathcal{L}M(t) \\ &\leq h(\hat{x}) - \mathcal{L}\|\hat{x} - x\| \\ &\leq h(\hat{x}) - |h(\hat{x}) - h(x)| \\ &\leq h(x), \end{aligned} \tag{55}$$

where we used (51), (28) and (49). □

Remark 1. For output feedback, the safety condition modifies from (43) to (52), that includes the extra robustifying term $\mathcal{L}\left(\dot{M}(t) + \gamma M(t)\right)$ to account for observer estimation errors. Agrawal and Panagou (2023) highlighted that if the observer satisfies $\dot{M}(t) \leq -\gamma M(t)$, then

$$L_{\hat{f}} h(\hat{x}, r, y) + L_{\hat{g}} h(\hat{x}, r, y)u \geq -\gamma h(\hat{x}) \tag{56}$$

is a sufficient condition for (52), i.e., the extra robustifying term can be dropped. For example, the Luenberger observer (26) associated with the linear system (10) and error bound (29) satisfies $\dot{M}(t) \leq -\gamma M(t)$ if $\lambda \geq \gamma$. This means that, if the observer is fast enough (characterized by λ) compared to how fast the system is allowed to approach the boundary of the safe set (expressed by γ), (56) guarantees safety. This idea first appeared in Molnar et al. (2021) and Singletary et al. (2022), where safety with exponentially stable tracking controllers was established similarly to our case of safety with exponentially stable observers. Furthermore, notice that condition $\hat{x}_0 \in \hat{C}(0)$ must also hold for safety, that is stricter than $x_0 \in C$. Accordingly, the initial state must be located farther inside the safe set ($h(x_0) \gg 0$) in case of significant initial state estimation errors. Under such conditions, the observer converges to an accurate state estimate by the time the system may get into a safety-critical scenario, and safety is maintained.

In the context of STC, Theorem 2 leads to the following controller for the case of output feedback:

$$\begin{aligned} k(\hat{x}, r, y) = \underset{u \in \mathbb{R}, \sigma_i \geq 0}{\operatorname{argmin}} \; & |u - u_0|^2 + \sum_{i=1}^{N} p_i \sigma_i^2 \\ \text{s.t. CAV}'\text{s safety}: \quad & L_{\hat{f}} h_0(\hat{x}, r, y) + L_{\hat{g}} h_0(\hat{x}, r, y)u + \gamma_0 h_0(\hat{x}) - \mathcal{L}\left(\dot{M}(t) + \gamma_0 M(t)\right) \geq 0, \\ \text{HVs}'\text{ safety}: \quad & \begin{cases} L_{\hat{f}} \bar{h}_1(\hat{x}, r, y) + L_{\hat{g}} \bar{h}_1(\hat{x}, r, y)u + \gamma_1 \bar{h}_1(\hat{x}) - \mathcal{L}\left(\dot{M}(t) + \gamma_1 M(t)\right) + \sigma_1 \geq 0, \\ \quad \vdots \\ L_{\hat{f}} \bar{h}_N(\hat{x}, r, y) + L_{\hat{g}} \bar{h}_N(\hat{x}, r, y)u + \gamma_N \bar{h}_N(\hat{x}) - \mathcal{L}\left(\dot{M}(t) + \gamma_N M(t)\right) + \sigma_N \geq 0, \end{cases} \end{aligned} \tag{57}$$

analogously to (48).

4. Numerical results

In this section, we carry out numerical simulations to show the effectiveness of the proposed STC framework. We first describe the simulation setup, then show our main results which validate that the proposed STC (48) leads to smooth and safe traffic in scenarios where the nominal controller (15) could yield collisions. The parameters used for simulations are given in Table 1 and at the figures. Finally, we show the performance of STC in a real-world traffic scenario by using experimental data to drive the simulations.

4.1. Simulation setup

We simulate an STC setup that includes one head HV (HHV), one CAV, and two identical following HVs (HV-1 and HV-2). We consider two risky traffic scenarios that could cause rear-end collision:

- *Scenario 1*: HHV suddenly decelerates, which may endanger the safety of all vehicles. This could be caused, for example, by an aggressive cut-in of a vehicle from an adjacent lane, or due to an obstacle on the road.
- *Scenario 2*: HV-2 unexpectedly accelerates. Importantly, such accelerations of follower HVs could cause a naïve nominal CAV controller to respond with acceleration and collide with the HHV in front of it.

Table 1
Parameters used for the numerical simulations.

Vehicle	Variable	Symbol	Value	Unit
All	Equilibrium velocity	$v^\star$	20	m/s
	Equilibrium spacing	$s^\star$	20	m
	Braking limit	$a_{\min}$	−7	m/s^2
	Acceleration limit	$a_{\max}$	7	m/s^2
HVs	Speed limit	$v_{\max}$	40	m/s
	Standstill spacing	s_{st}	5	m
	Free flow spacing	s_{go}	35	m
	Model coefficients	a	0.6	1/s
		b	0.9	1/s
CAV	Gains of nominal controller	μ_1	−2	1/s^2
		μ_2	−2	1/s^2
		k_1	0.2	1/s
		k_2	0.2	1/s
		τ	1	s
	Parameters of safety filter	γ	10	1/s
		p	100	1/s^2

Table 2
Acceleration of vehicles in the two safety-critical traffic scenarios.

	HHV	CAV	HV1	HV2
Scenario 1	(58) with $a_{\text{H}} = 6$ m/s^2 $t_{\text{H}} = 3.3$ s	(14) for nominal controller (48) for STC	(60)	(60)
Scenario 2	0	(14) for nominal controller (48) for STC	(60)	(59)–(60) with $a_{\text{F}} = 6$ m/s^2 $t_{\text{F}} = 2.5$ s

Specifically, we prescribe the following motions for the vehicles. We assume that initially all the four vehicles drive at the equilibrium velocity $v^\star$ and with uniform equilibrium spacing $s^\star$. In Scenario 1, the HHV brakes harshly, then accelerates to recover its original speed, and finally cruises at constant speed:

$$\dot{v}_{-1}(t) = \begin{cases} -a_{\text{H}} & \text{if} \quad t \in [0, t_{\text{H}}], \\ a_{\text{H}} & \text{if} \quad t \in (t_{\text{H}}, 2t_{\text{H}}], \\ 0 & \text{otherwise.} \end{cases} \tag{58}$$

In Scenario 2, the HHV drives at constant speed, $\dot{v}_{-1}(t) \equiv 0$. In both scenarios, the CAV uses the nominal controller (14) with feedback gains that satisfy the head-to-tail sting-stability condition given by (17)–(18). This nominal controller will be incorporated into and compared with STC (48). In Scenario 1, both HVs obey the driver model (1) with specific expression given below in (60). In Scenario 2, the motion of HV-2 is modified to accelerate before driving according to the model:

$$\dot{v}_2(t) = \begin{cases} a_{\text{F}} & \text{if} \quad t \in [0, t_{\text{F}}], \\ F_2(s_2, \dot{s}_2, v_2) & \text{otherwise.} \end{cases} \tag{59}$$

The behavior of each vehicle in the two safety-critical scenarios is summarized in Table 2.

To capture the longitudinal dynamics of HVs, we use the optimal velocity model (OVM) originating from (Bando et al., 1998):

$$F_i(s_i, \dot{s}_i, v_i) = a\left(V\left(s_i\right) - v_i\right) + b\dot{s}_i, \tag{60}$$

where $V(s_i)$ is a piecewise continuous function that represents the spacing-dependent desired velocity of the human drivers. The coefficient a characterizes how human drivers accelerate to match their current speed v_i with the desired driving speed $V(s_i)$, whereas coefficient b represents how human drivers change their acceleration according to the speed difference $\dot{s}_i$ between themselves and their preceding vehicle. The OVM (60) can be linearized as (7) with parameters:

$$a_1 = aV'(s^\star), \quad a_2 = a + b, \quad a_3 = b. \tag{61}$$

We use a range policy $V(s)$ from (Zhang and Orosz, 2016) as:

$$V(s) = \begin{cases} 0, & s \le s_{\text{st}}, \\ \frac{v_{\max}}{2}\left(1 - \cos\left(\pi \frac{s - s_{\text{st}}}{s_{\text{go}} - s_{\text{st}}}\right)\right), & s_{\text{st}} < s < s_{\text{go}}, \\ v_{\max}, & s \ge s_{\text{go}}, \end{cases} \tag{62}$$

where $s_{\text{st}}, s_{\text{go}}, v_{\max}$ represent standstill spacing, free flow spacing and the speed limit, respectively.

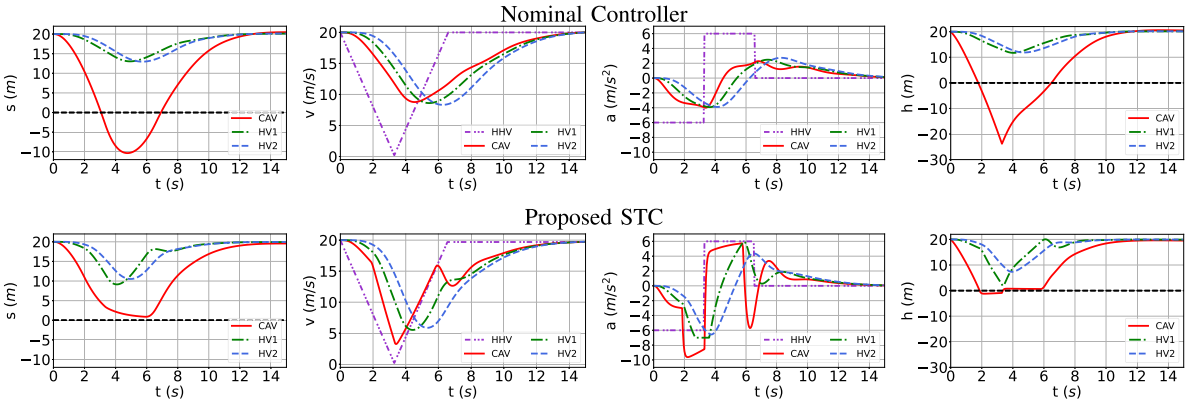

Fig. 3. Numerical simulation of the proposed safety-critical traffic controller (STC) in Scenario 1. The top row shows the behavior of mixed traffic when the CAV uses the nominal stabilizing controller (14). This achieves head-to-tail string stability (i.e., HV-2 reduces its speed less than the HHV) but yields unsafe behavior (i.e., the CAV collides with the HHV). The bottom row shows that the proposed STC (48) guarantees safety.

Our simulations focus on the case of two following HVs governed by the OVM, which is the simplest realization of the proposed STC. The design also works for larger numbers of HVs and other human driver models. This is demonstrated by simulation examples in Appendix. With this setup, we show that the proposed STC further provides safety guarantees for the mixed-autonomy traffic. Since the nominal controller (14) is designed based on the linear model (10), we synthesize the safety-critical controller by solving the QP (48) with $f(x,r) = Ax + Dr$ and $g(x) = B$ to compare with the nominal stabilization result in Wang et al. (2022a). When calculating the term $L_f \bar{h}$ in the QP (48), we treat the head vehicle's speed as external perturbation $r(t)$ and we omit the partial derivative of $\frac{\partial \bar{h}}{\partial r}\dot{r}$, since it is difficult in practice to obtain an accurate measurement of the head vehicle's acceleration $\dot{r}$ without connectivity. Although the QP (48) is formulated in continuous time, we solve it in a discrete time with a sampling time. Based on the typical information exchange rate of vehicle-to-vehicle communication (Torrent-Moreno et al., 2009), we set the sampling time as 0.05 s in Section 4.2 and as 0.1 s in Section 4.3.

4.2. Safety improvement by STC

Now we demonstrate by our main simulation results that the proposed STC improves the safety of mixed traffic. We highlight that while a nominal controller may lead to unsafe behavior when responding to sudden accelerations of human drivers, the STC maintains safety. In the simulations, we use the SDH safe spacing policy with CBF candidate (39) and parameters in Table 1. First, we consider full state feedback control in the two risky traffic situations described above (Scenario 1 and Scenario 2). We evaluate safety (i.e., whether the CBF candidates h_i and the spacings s_i stay positive over time) and head-to-tail string stability (i.e., whether the speed perturbations of the tail vehicle are smaller than those of the head vehicle).

Fig. 3 shows simulation results for Scenario 1, including the spacing s_i, velocity v_i, acceleration a_i and CBF candidate h_i of each vehicle for the cases of using the nominal controller (top) and the proposed STC (bottom). When the HHV suddenly reduces its speed, the nominal controller reduces the CAV's speed significantly less than the HHV does in order to achieve head-to-tail string stability. However, the CAV's deceleration ends up being too small, causing a collision between HHV and the CAV. This is indicated by $s_0 < 0$ along the red curve in Fig. 3. In contrast, with the proposed STC the CAV decelerates more and avoids collision with formal guarantees of safety. We remark that h_0 becomes slightly negative, which is caused by implementation inaccuracies (finite sampling time and neglecting $\frac{\partial \bar{h}}{\partial r}\dot{r}$). It should be noted that the HVs are collision-free and safe, although their safety was encoded as soft constraints in STC. Moreover, head-to-tail string stability is still achieved with STC, as HV-2 reduces its speed less than the HHV.

Fig. 4 presents simulation results for Scenario 2, by comparing the nominal controller (top) and STC (bottom). This scenario highlights that if a vehicle at the end of the chain accelerates, like HV-2 does, it can force the nominal controller of the CAV to accelerate and compromise the CAV's safety. By using STC, however, safe behavior is ensured for the CAV by the safety filter that is wrapped around the nominal controller.

In the results presented so far, the CAV's controller relies on the true state x and uses full state feedback. Now we address the scenario of output feedback, wherein the output y in (22) is available rather than the full state x. We use the state observer in (26) to establish an estimate $\hat{x}$ of the state (with initial estimate $\hat{x}_0 = [0, 0, 5, 5, 5, 0]^\top$). We compare two controllers:

- *"naïve" observer-based STC* that evaluates (48) with the estimated state $\hat{x}$, without considering the estimation error $\hat{x} - x$;
- *robust observer-based STC* (57) that takes into account the estimation error.

Fig. 5 shows simulation results for STC with observer in the naïve (top) and robust (bottom) implementations in Scenario 2 with $a_F = 6$ m/s^2 and $t_F = 2.2$ s. The figure highlights that the robust STC implementation leads to safer behavior (see the blue

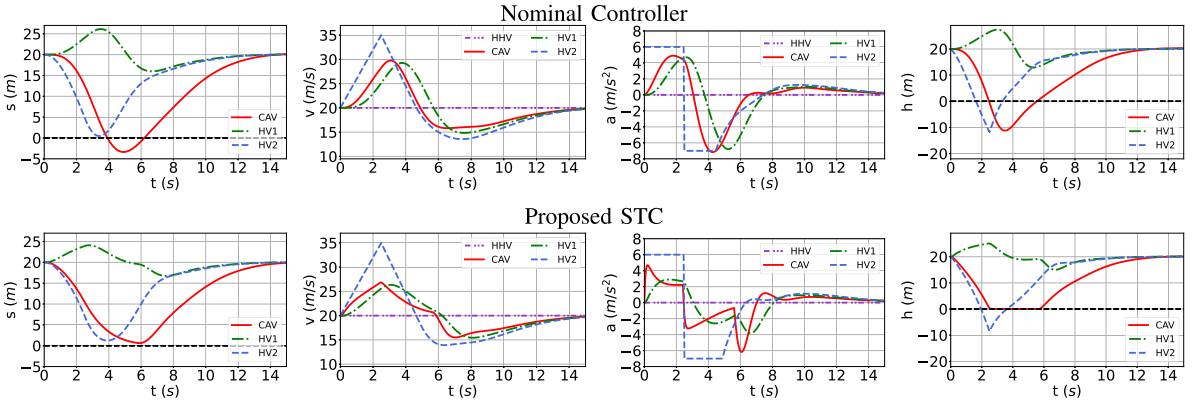

Fig. 4. Numerical simulation of Scenario 2. Similar to Fig. 3, this scenario highlights that certain behaviors of HVs can make the nominal controller of the CAV drive in an unsafe way (top), while the proposed STC recovers safe behavior (bottom).

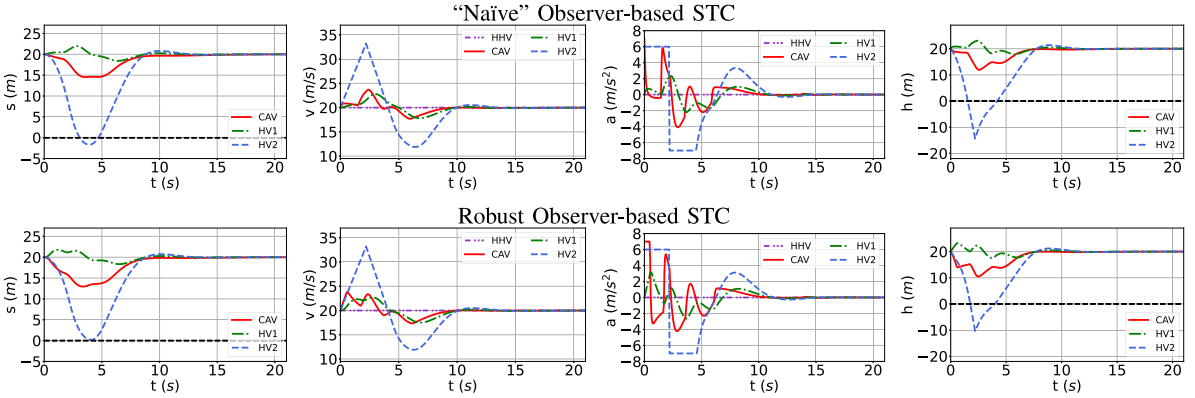

Fig. 5. Observer-based STC for guaranteed safety of mixed traffic with output feedback. A naïve implementation of observer-based STC (top), that disregards the observer's state estimation errors and directly evaluates (48) with the state estimated by the observer (26), can potentially cause safety violations. The robust implementation of observer-based STC (bottom), that takes into account the estimation error in (57), maintains formal safety guarantees.

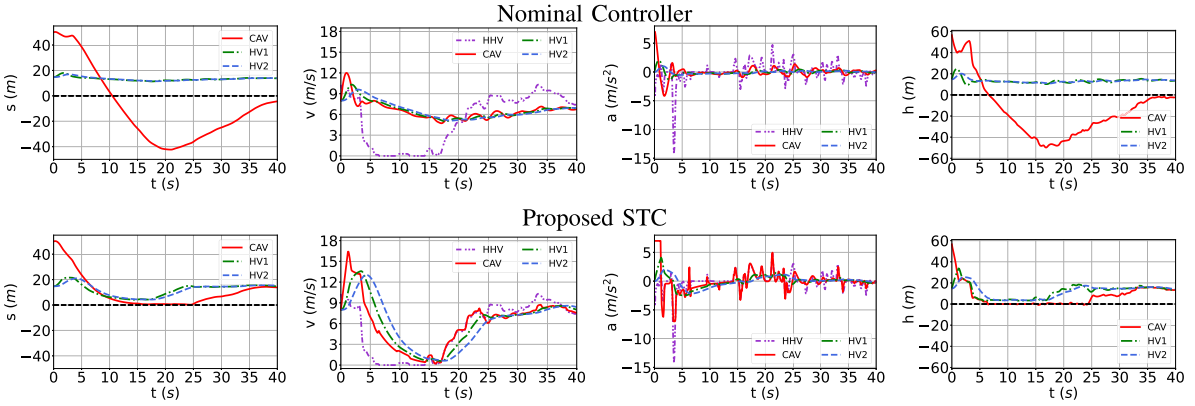

Fig. 6. Implementation of safety-critical traffic control (STC) in a real-world traffic scenario. The motion of the head HV is given by a trajectory from the NGSIM dataset, measured on highway I80 in California. Meanwhile the CAV and the following HVs are simulated, using the nominal controller (14) and the proposed STC (48). Remarkably, STC (bottom) is able to maintain safety when the head vehicle performs a harsh brake that happened in real life. This way, STC improves safety compared to the nominal controller (top), while leveraging the beneficial properties of this controller.

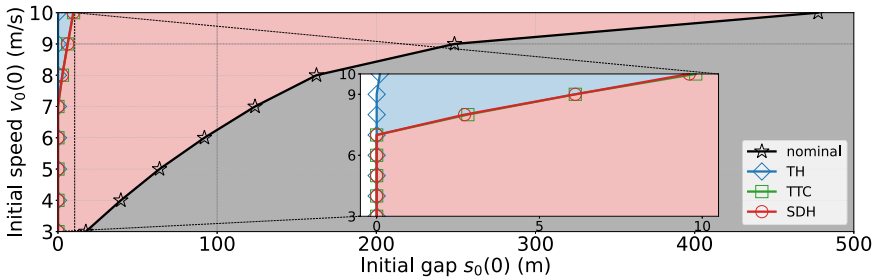

Fig. 7. Safety regions of the nominal controller and STC with three safe spacing policies, for the real-world traffic scenario presented in Fig. 6. If initial conditions are selected from the shaded domain (with gray, blue, green and red shadings for the cases of the nominal controller, and STC with the TH, TTC and SDH policies, respectively), then all vehicles avoid collision, even with limited acceleration capabilities. Clearly, the nominal controller requires large initial spacing to showcase safe behavior, while STC is able to prevent collisions for significantly smaller spacing.

Table 3
Parameters used for simulations driven by the NGSIM data.

Vehicle	Variable	Symbol	Value	Unit
All	Equilibrium velocity	$v^\star$	8	m/s
	Equilibrium spacing	$s^\star$	14.8	m
	Braking limit	$a_{\min}$	−7	m/s^2
	Acceleration limit	$a_{\max}$	7	m/s^2
HVs	Speed limit	$v_{\max}$	46.9	m/s
	Standstill spacing	s_{st}	1.6	m
	Free flow spacing	s_{go}	50	m
	Model coefficients	a	0.16	1/s
		b	0.63	1/s
CAV	Initial spacing	$s_0(0)$	50	m
	Gains of nominal controller	μ_1	−2	1/s^2
		μ_2	−2	1/s^2
		k_1	0.2	1/s
		k_2	0.2	1/s
		τ	3	s
	Parameters of safety filter	γ	10	1/s
		p	100	1/s^2

curves), thanks to taking into account the observer's estimation error bound in a provably safe fashion. As opposed, the naïve STC implementation no longer has formal safety guarantees when utilized with estimated state instead of true state.

While these results demonstrate the efficacy of STC, the Appendix provides a more extensive simulation study. These simulations address the effects of acceleration limits, as well as the choice of controller parameters and safe spacing policy.

4.3. Validation using NGSIM data

Finally, we demonstrate the applicability of STC to real-world traffic scenarios by using experimental data for the trajectory of the HHV while simulating the motions of the other vehicles.

We leverage the Next Generation Simulation (NGSIM) dataset that is widely used in transportation research. In particular, we use the reconstructed trajectory data from Montanino and Punzo (2015), that contains information about the motions of vehicles on highway I80 in Emeryville, California, including their position and speed as a function of time, with a resolution of 0.1 s. We select a vehicle (specifically, vehicle-2169) whose motion contains significant speed fluctuations, hence it poses a challenge for controlling a CAV behind it in a safety-critical fashion. The trajectory of this vehicle, including its speed and acceleration, is plotted in Fig. 6 by dashed purple line. Notice the abrupt braking at around $t = 4$ s, which can cause danger for the following vehicles. We use this speed profile as the speed of the HHV to simulate the motions of the CAV and the following HVs.

Fig. 6 presents simulation results that compare the nominal controller and STC (with the SDH policy). The simulation parameters of the OVM (60)–(62) are given in Table 3 (note that these were calibrated to the NGSIM dataset). The initial speeds of the CAV and the two HVs were set to $v_0(0) = v_1(0) = v_2(0) = v^\star$, and the initial spacings were chosen as $s_1(0) = s_2(0) = s^\star$ while $s_0(0)$ was set independently. The figure clearly reveals that the proposed STC framework is able to successfully modify the nominal controller and endow it with safe behavior, while the nominal controller on its own could cause collision between the CAV and the HHV. Importantly, the harsh braking of the HHV happened in real life, hence it is crucial to maintain safety guarantees while attempting to regulate the traffic flow with the motion of the CAV.

Finally, we further analyze to which extent STC improves safety. We repeat the simulation in Fig. 6 for various initial conditions. The motion of the HHV is kept the same (given by the experimental data), and the initial velocity $v_0(0)$ and initial spacing $s_0(0)$ of the

Table 4
Parameters used for the intelligent driver model.

Vehicle	Variable	Symbol	Value	Unit
HVs	Speed limit	v_0	36	m/s
	Standstill spacing	s_0	3.3	m
	Time headway	T	0.76	s
	Exponent	δ	6.13	–
	Maximum acceleration	a	2.43	m/s^2
	Deceleration coefficient	b	8.5	m/s^2

CAV are varied (while the rest of the initial conditions of HVs are determined by $v_0(0) = v_1(0) = v_2(0) = v^\star$ and $s_1(0) = s_2(0) = s^\star$). Fig. 7 shows the result of executing the nominal controller and STC with the three different safe spacing policies. For each case, thick lines with markers indicate the boundary of the shaded safety region where initial conditions are associated with collision-free motion for all vehicles. STC significantly enlarges the safety region of the nominal controller and, as a result, improves the safety of mixed traffic. Importantly, STC achieves this by incorporating and leveraging the nominal controller, while providing formal guarantees of safety.

5. Conclusions

In this paper, we proposed a safety-critical traffic control (STC) framework, in which the longitudinal motions of connected automated vehicles (CAVs) are regulated amongst human-driven vehicles (HVs) in mixed-autonomy traffic flows. The objective of STC is to guarantee safe, collision-free behavior. We formulated STC as a safety filter using control barrier functions (CBFs), that endows a nominal controller capable of attaining string stability with formal safety guarantees. We considered the safety of both the CAV and the following HVs. Moreover, we employed state observer-based CBFs to establish STC when the CAV does not have access to all the states of the following HVs. In our future work, we plan to address feedback, communication and actuation delays for the safety-critical control of mixed-autonomy traffic, and investigate control design for multiple CAVs.

Acknowledgments

This work was supported by National Natural Science Foundation of China under Project 62203131, Guangzhou Municipal-HKUST(GZ) joint Natural Science Foundation Research Project 2023A03J0149 and Guangzhou Municipal Science and Technology, China Project 2023A03J0011.

Appendix A. Effect of human driver model

In Section 4, we show that the STC enhances safety and avoids collision if we use the optimal velocity model (OVM) to describe human driver behavior. Now we demonstrate that STC also works for other choices of human driver model. We use intelligent driver model (IDM) as an example. The IDM describes the acceleration of HV-i as

$$F_i(s_i, \dot{s}_i, v_i) = a\left(1 - \left(\frac{v_i}{v_0}\right)^{\delta} - \left(\frac{s_0 + \max\left\{0, v_i T - \frac{v_i \dot{s}_i}{2\sqrt{ab}}\right\}}{s_i}\right)^2\right), \tag{63}$$

with the typical parameter values fitted to human driver data in Dollar et al. (2021), see Table 4.

The trajectories obtained by the nominal controller and STC are shown in Fig. 8 for Scenario 1. Similar to the OVM, we can conclude with the IDM that STC guarantees the safety of mixed traffic while the nominal controller could cause a collision.

Appendix B. Effect of number of following vehicles

In Section 4, we consider $N = 2$ following HVs to show that the STC enhances the safety of mixed traffic. Now we demonstrate the performance of STC for larger numbers of vehicles. Theoretically, the proposed STC works with guaranteed safety for any number N of following vehicles. Since STC is formulated as a quadratic program (48), it can be solved efficiently even for large numbers of constraints (corresponding to large numbers of vehicles). In practice, however, the size of the vehicle chain whose state the CAV may have access to is restricted by the range of the vehicle-to-vehicle communication. For example, the typical range of dedicated short range communication (DSRC) devices is a few hundred meters (Bai et al., 2010; Molnár et al., 2021). Considering $R = 300$ m communication range with our settings of equilibrium gap $s^* = 20$ m and vehicle length $l = 5$ m, this corresponds to a vehicle chain with at most $N = R/(s^* + l) = 12$ following vehicles.

We run simulations with $N = 12$ HVs governed by the OVM, and present the results in Fig. 9 for Scenario 1 and Fig. 10 for Scenario 2. We see that the STC maintains safety while the nominal controller causes a collision. For Scenario 1 (sudden deceleration of HHV), the size N of the vehicle chain has a marginal effect on safety, since the primary risk comes from the interaction of the

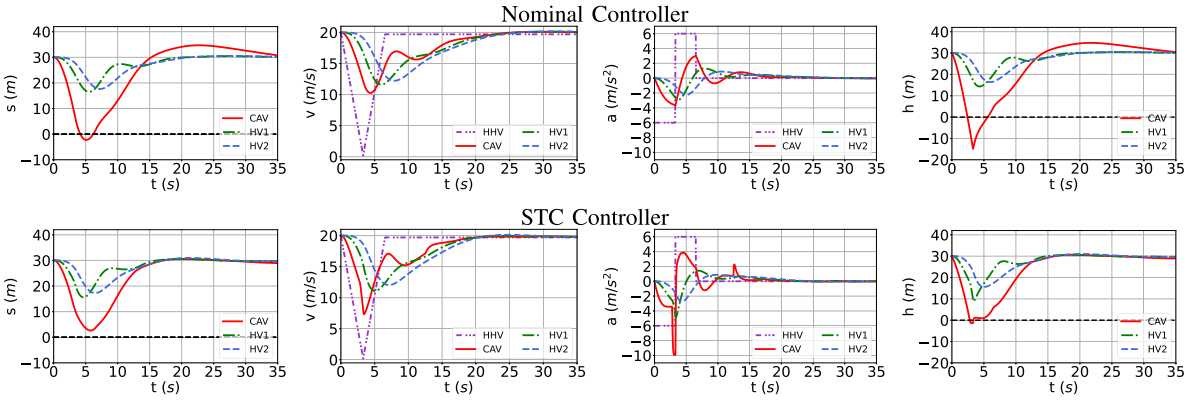

Fig. 8. Numerical simulations with the intelligent driver model (IDM) in Scenario 1. When the leading vehicle decelerates, the nominal controller (top) causes a collision for the CAV, while the proposed STC controller (bottom) guarantees safety.

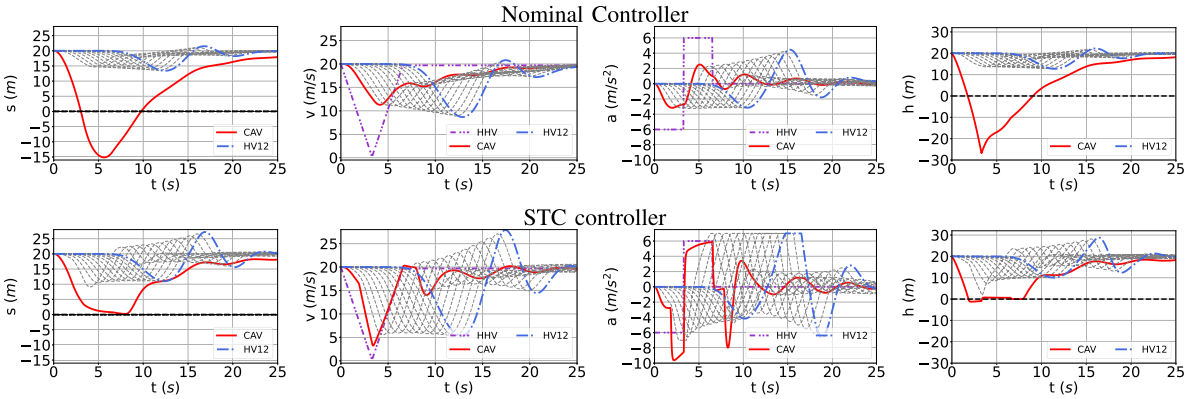

Fig. 9. Performance of STC when a mixed traffic including $N = 12$ HVs is controlled by the motion of a single CAV in Scenario 1. Safety guarantees are maintained despite the relatively large number of vehicles.

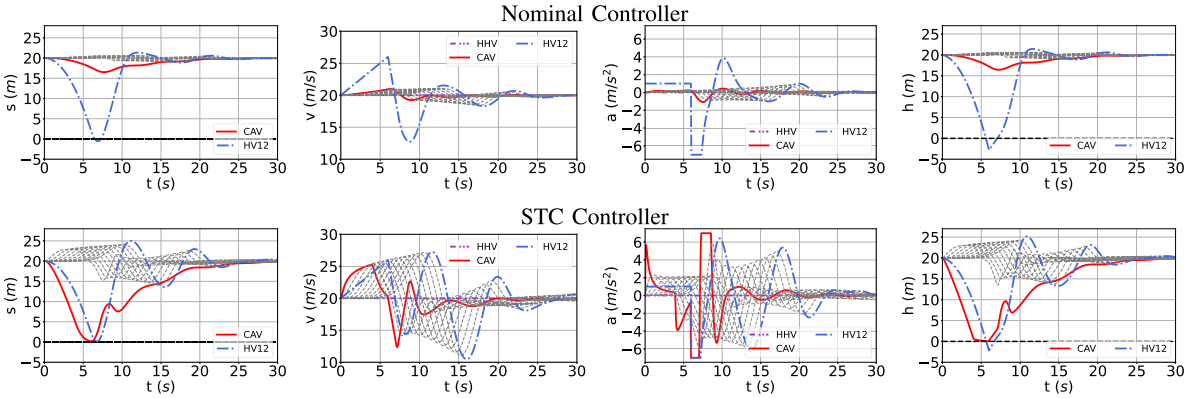

Fig. 10. Performance of STC with $N = 12$ HVs in Scenario 2. While the CAV is still guaranteed to be safe, it is more challenging to enhance the safety of the following HVs for such large number of vehicles.

CAV and HHV. However, the oscillations of the vehicle chain can increase with the number of vehicles. In other words, the STC controller might need to sacrifice more string stability in exchange for safety. For Scenario 2 (sudden acceleration of the last HV), it is expected that a larger number N of HVs implies a more challenging control problem for the CAV. When the CAV accelerates to help avoid collision between HV-N and HV-$(N-1)$, it takes time for the CAV's effect to propagate through the chain of following HVs. For smaller N, the propagation time is shorter, hence the STC is able to mitigate a collision. For larger N, the propagation time is longer, which may cause a collision before the following HVs begin to accelerate, and the STC may fail to assist the HVs in

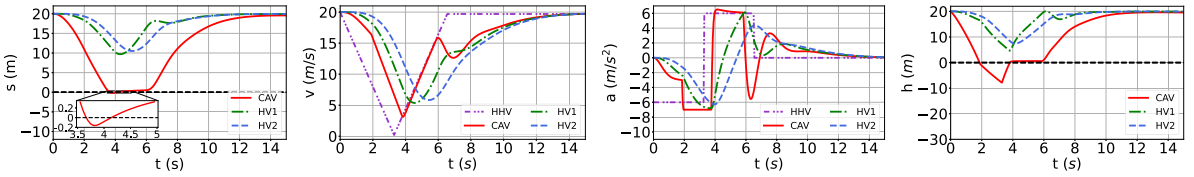

Fig. 11. The effect of acceleration limits on the performance of STC. The safety of mixed traffic is negatively impacted by the acceleration limits compared to the case with no limits shown at the bottom of Fig. 3.

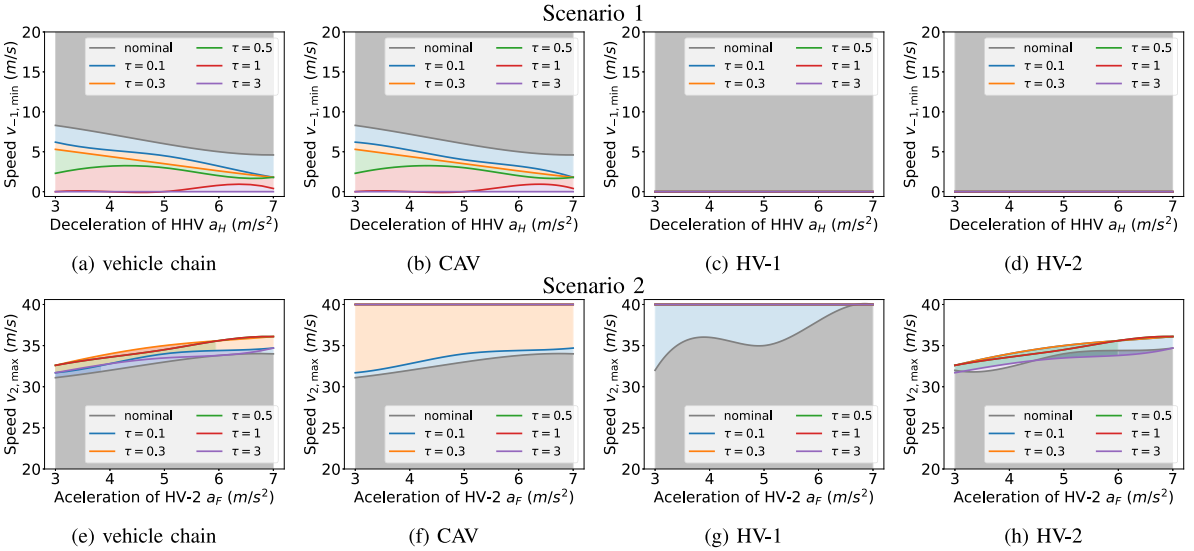

(a) vehicle chain (b) CAV (c) HV-1 (d) HV-2

(e) vehicle chain (f) CAV (g) HV-1 (h) HV-2

Fig. 12. The effect of speed and acceleration range of the perturbed HV on the safety of STC, as a function of parameter τ used in the SDH safe spacing policy. The gray shaded area is the range of speed perturbations to which the nominal controller responds safely, and the colored areas are the additional safety regions guaranteed by STC with different choice of τ. Remarkably, STC is able to keep the entire vehicle chain safe for a wide range of velocity perturbations, if a proper value of τ is chosen. For example, in the case of $\tau = 1$ s, the shaded safe region of STC covers most of the speed perturbations in panels (a)–(d), namely all speed and acceleration values combination in the region above the red-colored line.

collision avoidance. Hence, the acceleration allowed for the last following vehicle is smaller in the case of $N = 12$ in Fig. 10 than for $N = 2$ following vehicles in Fig. 4.

Appendix C. Analysis of STC parameters

In this part, we investigate the STC performance in more detail. We include a discussion about the effects of acceleration limits, the selection of parameters, and the choice of spacing policy. Through these, we highlight some limitations of the present approach and give suggestions on how to overcome them. For simplicity, we conduct this analysis for full state feedback without incorporating observers into the control loop.

First, we highlight that safety may be affected by the acceleration capabilities of vehicles. Notice that the control input u of the proposed STC (48) and the accelerations $\dot{v}_i$ obtained from the human driver model (60) can take any real value. In practice, however, vehicles have limited acceleration capabilities, hence these quantities are constrained to the range $[a_{i,\min}, a_{i,\max}]$. To investigate the effect of acceleration limits on safety, we conduct simulations where the accelerations are saturated as $\dot{v}_0 = \mathrm{sat}(u)$ and $\dot{v}_i = \mathrm{sat}\big(F_i\left(s_i, \dot{s}_i, v_i\right)\big)$, $i \in \{1, \dots, N\}$, with

$$\mathrm{sat}(u) = \max\big\{a_{\min}, \min\{u, a_{\max}\}\big\} \tag{64}$$

and uniform acceleration limits $a_{\min}$ and $a_{\max}$ for each vehicle given in Table 1.

Fig. 11 presents the effect of acceleration limits on safety. Here, the simulation scenario and parameters correspond to the bottom of Fig. 3, except that the saturation function is also incorporated into the dynamics. The red curves in the figure highlight that there exist scenarios in which acceleration limits affect safety (i.e., s_0 goes negative when the acceleration of the CAV saturates), since these limits are not incorporated into the STC design. While addressing bounded control inputs (limited acceleration) is possible by CBF theory (Gurriet et al., 2020; Agrawal and Panagou, 2021; Liu et al., 2023) and could be included in STC, it is a nontrivial task and greatly increases the complexity of control design—hence it is left for future work. Instead, in this paper, we quantify the amount of safety violations due to the saturation, and tune the controller parameters to eliminate these violations.

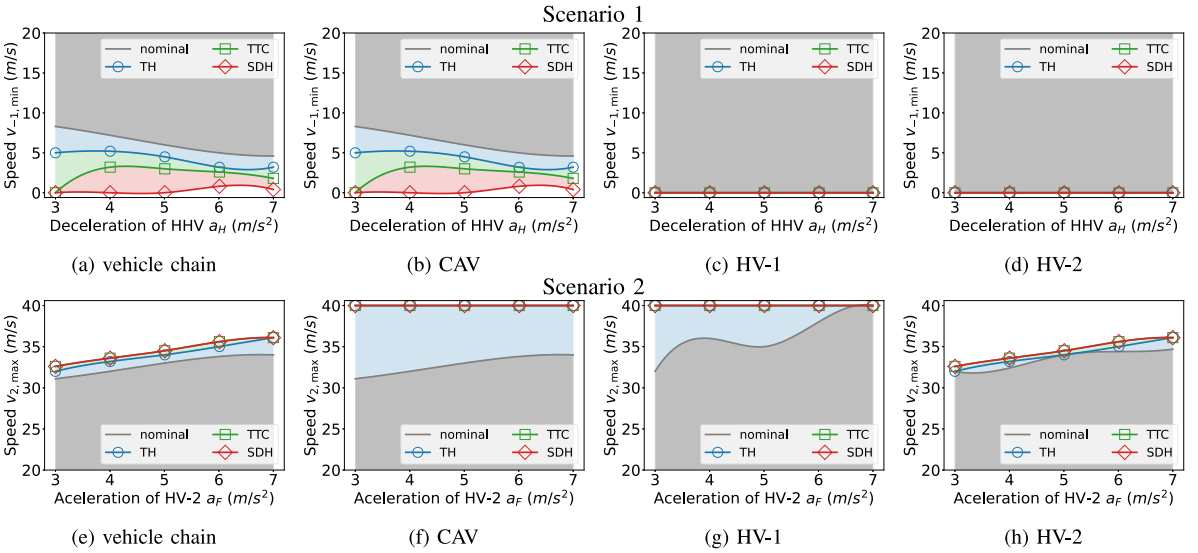

Fig. 13. Comparison of STC implemented with the time headway (TH), time-to-collision (TTC) and stopping distance headway (SDH) safe spacing policies given in (30)–(32), using the metrics introduced in Fig. 12.

Specifically, we investigate the effects of three main sets of tunable parameters in STC (48): the time τ_i in the CBF candidates, the coefficient γ_i in the safety constraints, and the penalty p_i in the cost. For simplicity, we keep these parameters to be the same for all vehicles, and we use the short notation τ, γ, p. The default values of these parameters (used in the previous figures) are listed in Table 1. Now we analyze how these parameters affect the performance of STC.

In particular, we characterize how abrupt HV motions can be handled by STC with limited acceleration as a function of parameters τ, γ, p. To achieve this, we conduct a large number of simulations with various a_{H}, t_{H}, a_{F}, t_{F} values characterizing the motion of the HVs in (58)–(59). In Scenario 1, we quantify how much the HHV can reduce its speed without causing collision, i.e., we identify the safe range of the minimum speed $v_{-1,\min} = v^\star - a_{\mathrm{H}} t_{\mathrm{H}}$ for which the response of the vehicles satisfies $s_i(t) \geq 0$. In Scenario 2, we quantify how much HV-2 can increase its speed without causing collision, i.e., we calculate the safe range of $v_{2,\max} = v^\star + a_{\mathrm{F}} t_{\mathrm{F}}$ for which $s_i(t) \geq 0$. We calculate these by considering both the entire vehicle chain (such that $s_i(t) \geq 0$, $\forall i \in \{0, 1, 2\}$), and also separately for the CAV ($s_0(t) \geq 0$), HV-1 ($s_1(t) \geq 0$) and HV-2 ($s_2(t) \geq 0$).

Fig. 12 shows the safe regions of $v_{-1,\min}$ in Scenario 1 (top) and $v_{2,\max}$ in Scenario 2 (bottom) for various accelerations a_{H} and a_{F}, respectively. These results are presented for fixed γ and p, while varying τ. We make the following conclusions.

- In Scenario 1, there is no collision for HV-1 and HV-2 for all values of τ even if the HHV brakes to a complete stop, since the safe range of $v_{-1,\min}$ covers the whole interval $[0, v^\star]$ in Fig. 12(c) and (d). The safety of the vehicle chain is therefore determined by the safety of the CAV. Considering the CAV's safety in Fig. 12(b), the safe range of $v_{-1,\min}$ grows by increasing τ, since larger τ corresponds to larger safe spacing. Ultimately, STC makes the CAV avoid collisions for any HHV motion if τ is selected to be large enough—even with limited acceleration capability.
- In Scenario 2, the CAV still avoids collision with STC if τ is large enough. According to Fig. 12(f), the safe range of $v_{2,\max}$ covers the whole interval $[v^\star, v_{\max}]$ for almost all choices of τ except the smallest value. The trend is the opposite for HV-2, where the safe range of $v_{2,\max}$ shrinks for the largest value of τ; see panel (h). Meanwhile, HV-1 avoids collision for any τ; see panel (g).

Moreover, notice that STC (in color) outperforms the nominal controller (gray) in both scenarios, since the safe ranges of $v_{-1,\min}$ and $v_{2,\max}$ are significantly larger for STC. That is, STC is able to avoid collision even for large speed perturbations, including cases when the head vehicle decelerates to zero speed, while this may not be achieved by linear controllers like (14). Importantly, Lunze (2019) also highlighted that linear controllers could fail to stabilize the traffic or to avoid a collision in case of large perturbations from the equilibrium states. STC, on the other hand, showcases collision-free behavior even though it was designed based on a linear model and evaluated for the nonlinear dynamics in this example. Finally, we performed the same analysis by varying γ in the range $\gamma \in \{5, 10, 15\}$ while keeping τ and p fixed, and by varying p in the range $p \in \{10, 100, 1000\}$ while keeping τ and γ fixed. We found that the STC is less sensitive to γ and p, as there is only slight variation in the safe ranges of velocity perturbations. These analyses justify the parameter selection in Table 1.

Collision-free behavior not only depends on the parameters of the controller but also on the safe spacing policy implemented. So far, we showed results for the case of the SDH policy only. Now we compare the TH (30), TTC (31) and SDH (32) safe spacing policies. While there has been related research comparing the TH and TTC policies (Vogel, 2003), a detailed comparison of these in the context of safety-critical traffic control have not yet been investigated.

Fig. 13 shows the safe ranges of HV velocity perturbations using the different safe spacing policies. Considering the entire vehicle chain, we find that the safe region of the SDH policy is larger than those of the other two policies in Scenario 1, and the difference between the three policies is negligible in Scenario 2. This showcases the ability of the proposed STC framework to accommodate various spacing policies.

References

Abduljabbar, M., Meskin, N., Cassandras, C.G., 2021. Control barrier function-based lateral control of autonomous vehicle for roundabout crossing. In: IEEE International Conference on Intelligent Transportation Systems. pp. 859–864.

Agrawal, Devansh R., Panagou, Dimitra, 2021. Safe control synthesis via input constrained control barrier functions. In: 60th IEEE Conference on Decision and Control. pp. 6113–6118.

Agrawal, Devansh R., Panagou, Dimitra, 2023. Safe and robust observer-controller synthesis using control barrier functions. IEEE Control Syst. Lett. 7, 127–132.

Alam, Assad, Gattami, Ather, Johansson, Karl H., Tomlin, Claire J., 2014. Guaranteeing safety for heavy duty vehicle platooning: Safe set computations and experimental evaluations. Control Eng. Pract. 24, 33–41.

Alan, Anil, Taylor, Andrew J., He, Chaozhe R., Ames, Aaron D., Orosz, Gabor, 2022. Control barrier functions and input-to-state safety with application to automated vehicles. arXiv preprint, arXiv:2206.03568.

Almubarak, Hassan, Theodorou, Evangelos A., Sadegh, Nader, 2021. HJB based optimal safe control using control barrier functions. In: IEEE Conference on Decision and Control. IEEE, pp. 6829–6834.

Ames, Aaron D., Coogan, Samuel, Egerstedt, Magnus, Notomista, Gennaro, Sreenath, Koushil, Tabuada, Paulo, 2019. Control barrier functions: Theory and applications. In: European Control Conference. IEEE, pp. 3420–3431.

Ames, Aaron D., Grizzle, Jessy W., Tabuada, Paulo, 2014. Control barrier function based quadratic programs with application to adaptive cruise control. In: IEEE Conference on Decision and Control. IEEE, pp. 6271–6278.

Arvin, Ramin, Khattak, Asad J., Kamrani, Mohsen, Rio-Torres, Jackeline, 2020. Safety evaluation of connected and automated vehicles in mixed traffic with conventional vehicles at intersections. J. Intell. Transp. Syst. 25 (2), 170–187.

Avedisov, S.S., Bansal, G., Orosz, G., 2022. Impacts of connected automated vehicles on freeway traffic patterns at different penetration levels. IEEE Trans. Intell. Transp. Syst. 5 (23), 4305–4318.

Bai, Fan, Stancil, Daniel D., Krishnan, Hariharan, 2010. Toward understanding characteristics of dedicated short range communications (DSRC) from a perspective of vehicular network engineers. In: 16th Annual International Conference on Mobile Computing and Networking. pp. 329–340.

Bando, Masako, Hasebe, Katsuya, Nakanishi, Ken, Nakayama, Akihiro, 1998. Analysis of optimal velocity model with explicit delay. Phys. Rev. E 58 (5), 5429.

Callier, Frank M., Desoer, Charles A., 2012. Linear System Theory. Springer Science & Business Media.

Chen, Yuxiao, Peng, Huei, Grizzle, Jessy, 2018. Obstacle avoidance for low-speed autonomous vehicles with barrier function. IEEE Trans. Control Syst. Technol. 26 (1), 194–206.

Čičić, Mladen, Johansson, Karl Henrik, 2018. Traffic regulation via individually controlled automated vehicles: a cell transmission model approach. In: IEEE International Conference on Intelligent Transportation Systems. IEEE, pp. 766–771.

Čičić, Mladen, Xiong, Xi, Jin, Li, Johansson, Karl Henrik, 2022. Coordinating vehicle platoons for highway bottleneck decongestion and throughput improvement. IEEE Trans. Intell. Transp. Syst. 23 (7), 8959–8971.

Cui, Shumo, Seibold, Benjamin, Stern, Raphael, Work, Daniel B., 2017. Stabilizing traffic flow via a single autonomous vehicle: Possibilities and limitations. In: IEEE Intelligent Vehicles Symposium. IEEE, pp. 1336–1341.

Dollar, R. Austin, Molnár, Tamás G., Vahidi, Ardalan, Orosz, Gábor, 2021. MPC-based connected cruise control with multiple human predecessors. In: American Control Conference. IEEE, pp. 405–411.

Feng, Shuo, Zhang, Yi, Li, Shengbo Eben, Cao, Zhong, Liu, Henry X., Li, Li, 2019. String stability for vehicular platoon control: Definitions and analysis methods. Annu. Rev. Control 47, 81–97.

Ge, J.I., Avedisov, S.S., He, C.R., Qin, W.B., Sadeghpour, M., Orosz, G., 2018. Experimental validation of connected automated vehicle design among human-driven vehicles. Transp. Res. C 91, 335–352.

Gunter, George, Nice, Matthew, Bunting, Matt, Sprinkle, Jonathan, Work, Daniel B., 2022. Experimental testing of a control barrier function on an automated vehicle in live multi-lane traffic. In: Workshop on Data-Driven and Intelligent Cyber-Physical Systems for Smart Cities. pp. 31–35.

Gunter, George, Stern, Raphael, Work, Daniel B., 2019. Modeling adaptive cruise control vehicles from experimental data: model comparison. In: IEEE Conference on Intelligent Transportation Systems. IEEE, pp. 3049–3054.

Gurriet, T., Mote, M., Singletary, A., Nilsson, P., Feron, E., Ames, A.D., 2020. A scalable safety critical control framework for nonlinear systems. IEEE Access 8, 187249–187275.

Horowitz, Roberto, May, Adolf, Skabardonis, Alex, Varaiya, Pravin, Zhang, Michael, Gomes, Gabriel, Munoz, Laura, Sun, Xiaotian, Sun, Dengfeng, 2005. Design, Field Implementation and Evaluation of Adaptive Ramp Metering Algorithms. Technical report, California PATH Research Report UCB-ITS-PRR-2005-2.

Huang, Kuang, Di, Xuan, Du, Qiang, Chen, Xi, 2020. Scalable traffic stability analysis in mixed-autonomy using continuum models. Transp. Res. C 111, 616–630.

Jankovic, Mrdjan, Santillo, Mario, Wang, Yan, 2022. Multi-agent systems with CBF-based controllers – collision avoidance and liveness from instability. arXiv preprint, arXiv:2207.04915.

Jovanović, Mihailo R., Dhingra, Neil K., 2016. Controller architectures: Tradeoffs between performance and structure. Eur. J. Control 30, 76–91.

Kesting, Arne, Treiber, Martin, Helbing, Dirk, 2010. Enhanced intelligent driver model to access the impact of driving strategies on traffic capacity. Phil. Trans. R. Soc. A 368 (1928), 4585–4605.

Krstic, Miroslav, 2021. Inverse optimal safety filters. arXiv preprint, arXiv:2112.08225.

Li, Xiaopeng, 2022. Trade-off between safety, mobility and stability in automated vehicle following control: An analytical method. Transp. Res. B 166, 1–18.

Li, Xiaopeng, Cui, Jianxun, An, Shi, Parsafard, Mohsen, 2014. Stop-and-go traffic analysis: Theoretical properties, environmental impacts and oscillation mitigation. Transp. Res. B 70, 319–339.

Li, Ye, Wang, Hao, Wang, Wei, Xing, Lu, Liu, Shanwen, Wei, Xueyan, 2017a. Evaluation of the impacts of cooperative adaptive cruise control on reducing rear-end collision risks on freeways. Accid. Anal. Prev. 98, 87–95.

Li, Shengbo Eben, Zheng, Yang, Li, Keqiang, Wu, Yujia, Hedrick, J. Karl, Gao, Feng, Zhang, Hongwei, 2017b. Dynamical modeling and distributed control of connected and automated vehicles: Challenges and opportunities. IEEE Intell. Transp. Syst. Mag. 9 (3), 46–58.

Liu, Simin, Liu, Changliu, Dolan, John, 2023. Safe control under input limits with neural control barrier functions. In: Conference on Robot Learning. PMLR, pp. 1970–1980.

Luenberger, David, 1971. An introduction to observers. IEEE Trans. Automat. Control 16 (6), 596–602.

Lunze, Jan, 2019. Adaptive cruise control with guaranteed collision avoidance. IEEE Trans. Intell. Transp. Syst. 20 (5), 1897–1907.

Makridis, Michail, Mattas, Konstantinos, Ciuffo, Biagio, 2019. Response time and time headway of an adaptive cruise control. An empirical characterization and potential impacts on road capacity. IEEE Trans. Intell. Transp. Syst. 21 (4), 1677–1686.

Marsden, Greg, McDonald, Mike, Brackstone, Mark, 2001. Towards an understanding of adaptive cruise control. Transp. Res. C 9 (1), 33–51.

Massera Filho, Carlos, Terra, Marco H., Wolf, Denis F., 2017. Safe optimization of highway traffic with robust model predictive control-based cooperative adaptive cruise control. IEEE Trans. Intell. Transp. Syst. 18 (11), 3193–3203.
Milanés, Vicente, Shladover, Steven E., Spring, John, Nowakowski, Christopher, Kawazoe, Hiroshi, Nakamura, Masahide, 2013. Cooperative adaptive cruise control in real traffic situations. IEEE Trans. Intell. Transp. Syst. 15 (1), 296–305.
Molnar, Tamas G., Cosner, Ryan K., Singletary, Andrew W., Ubellacker, Wyatt, Ames, Aaron D., 2021. Model-free safety-critical control for robotic systems. IEEE Robot. Autom. Lett. 7 (2), 944–951.
Molnár, Tamás G., Hopka, Michael, Upadhyay, Devesh, Van Nieuwstadt, Michiel, Orosz, Gábor, 2023. Virtual rings on highways: Traffic control by connected automated vehicles. In: AI-Enabled Technologies for Autonomous and Connected Vehicles. Springer, pp. 441–479.
Molnár, Tamás G., Upadhyay, Devesh, Hopka, Michael, Van Nieuwstadt, Michiel, Orosz, Gábor, 2020. Open and closed loop traffic control by connected automated vehicles. In: IEEE Conference on Decision and Control. pp. 239–244.
Molnár, Tamás G., Upadhyay, Devesh, Hopka, Michael, Van Nieuwstadt, Michiel, Orosz, Gábor, 2021. Delayed Lagrangian continuum models for on-board traffic prediction. Transp. Res. C 123, 102991.
Montanino, Marcello, Punzo, Vincenzo, 2015. Trajectory data reconstruction and simulation-based validation against macroscopic traffic patterns. Transp. Res. B 80, 82–106.
Monteiro, Fernando V., Ioannou, Petros, 2023. Safe autonomous lane changes and impact on traffic flow in a connected vehicle environment. Transp. Res. C 151, 104138.
Morando, Mark Mario, Tian, Qingyun, Truong, Long T., Vu, Hai L., 2018. Studying the safety impact of autonomous vehicles using simulation-based surrogate safety measures. J. Adv. Transp. 2018, 6135183.
Nguyen, Quan, Sreenath, Koushil, 2016. Exponential control barrier functions for enforcing high relative-degree safety-critical constraints. In: American Control Conference. IEEE, pp. 322–328.
Orosz, Gábor, 2016. Connected cruise control: modelling, delay effects, and nonlinear behaviour. Veh. Syst. Dyn. 54 (8), 1147–1176.
Rahman, Md. Sharikur, Abdel-Aty, Mohamed, 2018. Longitudinal safety evaluation of connected vehicles' platooning on expressways. Accid. Anal. Prev. 117, 381–391.
Rios-Torres, Jackeline, Malikopoulos, Andreas A., 2018. Impact of partial penetrations of connected and automated vehicles on fuel consumption and traffic flow. IEEE Trans. Intell. Veh. 3 (4), 453–462.
Ro, Jin Woo, Roop, Partha S., Malik, Avinash, 2020. A new safety distance calculation for rear-end collision avoidance. IEEE Trans. Intell. Transp. Syst. 22 (3), 1742–1747.
Shang, Mingfeng, Stern, Raphael E., 2021. Impacts of commercially available adaptive cruise control vehicles on highway stability and throughput. Transp. Res. C 122, 102897.
Shi, Xiaowei, Li, Xiaopeng, 2021. Empirical study on car-following characteristics of commercial automated vehicles with different headway settings. Transp. Res. C 128, 103134.
Singletary, Andrew, Guffey, William, Molnar, Tamas G., Sinnet, Ryan, Ames, Aaron D., 2022. Safety-critical manipulation for collision-free food preparation. IEEE Robot. Autom. Lett. 7 (4), 10954–10961.
Stern, Raphael E., Cui, Shumo, Delle Monache, Maria Laura, Bhadani, Rahul, Bunting, Matt, Churchill, Miles, Hamilton, Nathaniel, Pohlmann, Hannah, Wu, Fangyu, Piccoli, Benedetto, et al., 2018. Dissipation of stop-and-go waves via control of autonomous vehicles: Field experiments. Transp. Res. C 89, 205–221.
Talebpour, Alireza, Mahmassani, Hani S., 2016. Influence of connected and autonomous vehicles on traffic flow stability and throughput. Transp. Res. C 71, 143–163.
Torrent-Moreno, Marc, Mittag, Jens, Santi, Paolo, Hartenstein, Hannes, 2009. Vehicle-to-vehicle communication: Fair transmit power control for safety-critical information. IEEE Trans. Veh. Technol. 58 (7), 3684–3703.
Treiber, Martin, Kesting, Arne, 2013. Traffic Flow Dynamics: Data, Models and Simulation. Springer-Verlag, Berlin.
Vahidi, Ardalan, Sciarretta, Antonio, 2018. Energy saving potentials of connected and automated vehicles. Transp. Res. C 95, 822–843.
Vogel, Katja, 2003. A comparison of headway and time to collision as safety indicators. Accid. Anal. Prev. 35 (3), 427–433.
Wang, Yujie, Xu, Xiangru, 2022. Observer-based control barrier functions for safety critical systems. In: American Control Conference. pp. 709–714.
Wang, Jiawei, Zheng, Yang, Chen, Chaoyi, Xu, Qing, Li, Keqiang, 2022a. Leading cruise control in mixed traffic flow: System modeling, controllability, and string stability. IEEE Trans. Intell. Transp. Syst. 23 (8), 12861–12876.
Wang, Jiawei, Zheng, Yang, Li, Keqiang, Xu, Qing, 2022b. DeeP-LCC: Data-enabled predictive leading cruise control in mixed traffic flow. arXiv preprint, arXiv:2203.10639.
Wang, Jiawei, Zheng, Yang, Xu, Qing, Li, Keqiang, 2022c. Data-driven predictive control for connected and autonomous vehicles in mixed traffic. In: American Control Conference. pp. 4739–4745.
Wang, Jiawei, Zheng, Yang, Xu, Qing, Wang, Jianqiang, Li, Keqiang, 2020. Controllability analysis and optimal control of mixed traffic flow with human-driven and autonomous vehicles. IEEE Trans. Intell. Transp. Syst. 22 (12), 7445–7459.
Wu, Cathy, Kreidieh, Abdul Rahman, Parvate, Kanaad, Vinitsky, Eugene, Bayen, Alexandre M., 2022. Flow: A modular learning framework for mixed autonomy traffic. IEEE Trans. Robot. 38 (2), 1270–1286.
Xiao, Wei, Belta, Calin, 2022. High order control barrier functions. IEEE Trans. Automat. Control 67 (7), 3655–3662.
Xiao, Wei, Belta, Calin, Cassandras, Christos G., 2019. Decentralized merging control in traffic networks: A control barrier function approach. In: ACM/IEEE International Conference on Cyber-Physical Systems. pp. 270–279.
Xu, Xiangru, 2018. Constrained control of input–output linearizable systems using control sharing barrier functions. Automatica 87, 195–201.
Ye, Lanhang, Yamamoto, Toshiyuki, 2019. Evaluating the impact of connected and autonomous vehicles on traffic safety. Phys. A 526, 121009.
Yu, Huan, Koga, Shumon, Krstic, Miroslav, 2018. Stabilization of traffic flow with a leading autonomous vehicle. In: Dynamic Systems and Control Conference, Vol. 51906. American Society of Mechanical Engineers, V002T22A006.
Yu, Huan, Krstic, Miroslav, 2019. Traffic congestion control for Aw–Rascle–Zhang model. Automatica 100, 38–51.
Zhang, Yihang, Ioannou, Petros A., 2016. Combined variable speed limit and lane change control for highway traffic. IEEE Trans. Intell. Transp. Syst. 18 (7), 1812–1823.
Zhang, Linjun, Orosz, Gábor, 2016. Motif-based design for connected vehicle systems in presence of heterogeneous connectivity structures and time delays. IEEE Trans. Intell. Transp. Syst. 17 (6), 1638–1651.
Zhang, Liguo, Prieur, Christophe, Qiao, Junfei, 2019. PI boundary control of linear hyperbolic balance laws with stabilization of ARZ traffic flow models. Systems Control Lett. 123, 85–91.
Zheng, Yang, Li, Shengbo Eben, Li, Keqiang, Borrelli, Francesco, Hedrick, J. Karl, 2016. Distributed model predictive control for heterogeneous vehicle platoons under unidirectional topologies. IEEE Trans. Control Syst. Technol. 25 (3), 899–910.
Zheng, Yang, Li, Shengbo Eben, Wang, Jianqiang, Cao, Dongpu, Li, Keqiang, 2015. Stability and scalability of homogeneous vehicular platoon: Study on the influence of information flow topologies. IEEE Trans. Intell. Transp. Syst. 17 (1), 14–26.
Zheng, Yang, Wang, Jiawei, Li, Keqiang, 2020. Smoothing traffic flow via control of autonomous vehicles. IEEE Internet Things J. 7 (5), 3882–3896.
Zhou, Jingyuan, Yu, Huan, 2022. Safety critical control of mixed-autonomy traffic via a single autonomous vehicle. In: 2022 IEEE 25th International Conference on Intelligent Transportation Systems. ITSC, IEEE, pp. 3089–3094.
Zhu, Wen-Xing, Zhang, H.M., 2018. Analysis of mixed traffic flow with human-driving and autonomous cars based on car-following model. Phys. A 496, 274–285.
Zhu, Yang, Zhu, Feng, 2019. Barrier-function-based distributed adaptive control of nonlinear CAVs with parametric uncertainty and full-state constraint. Transp. Res. C 104, 249–264.